Drug-target Mendelian randomization analysis supports lowering plasma ANGPTL3, ANGPTL4, and APOC3 levels as strategies for reducing cardiovascular disease risk

Fredrik Landfors[1, 2, *], Peter Henneman[3], Elin Chorell[1], Stefan K. Nilsson[2, 4], Sander Kersten[5, 6]

[1] Department of Public Health and Clinical Medicine, Section of Medicine, Umea University, S-901 87 Umea, Sweden.

[2] Lipigon Pharmaceuticals AB, S-907 36 Umea, Sweden.

[3] Department of Human Genetics, Amsterdam University Medical Center, Meibergdreef 9, 1105 AZ, Amsterdam, The Netherlands.

[4] Department of Medical Biosciences, Umea University, S-901 87 Umea, Sweden.

[5] Nutrition, Metabolism, and Genomics group, Division of Human Nutrition and Health, Wageningen University, 6708WE, Wageningen, the Netherlands.

[6] Division of Nutritional Sciences, Cornell University, Ithaca, NY 14853, USA.

[*] To whom correspondence should be addressed.

Contact information for the corresponding author: Fredrik Landfors, Department of Public Health and Clinical Medicine, Umea University, S-901 87 Umea, Sweden; Email: Fredrik.Landfors@umu.se; Phone: +46 (0) 70-454 92 08.

ABSTRACT

Background and Aims: APOC3, ANGPTL3, and ANGPTL4 are circulating proteins that are actively pursued as pharmacological targets to treat dyslipidemia and reduce the risk of atherosclerotic cardiovascular disease. Here, we used human genetic data to compare the predicted therapeutic and adverse effects of APOC3, ANGPTL3, and ANGPTL4 inactivation.

Methods: We conducted drug-target Mendelian randomization analyses using variants in proximity to the genes associated with circulating protein levels to compare APOC3, ANGPTL3, and ANGPTL4 as drug targets. We obtained exposure and outcome data from large-scale genome-wide association studies and used generalized least squares to correct for linkage disequilibrium-related correlation. We evaluated five primary cardiometabolic endpoints and screened for potential side effects across 694 disease-related endpoints, 43 clinical laboratory tests, and 11 internal organ MRI measurements.

Results: Genetically lowering circulating ANGPTL4 levels reduced the odds of coronary artery disease (CAD) (odds ratio, 0.57 per s.d. protein [95%CI,0.47–0.70]) and type 2 diabetes (T2D) (odds ratio, 0.73 per s.d. protein [95%CI,0.57–0.94]). Genetically lowering circulating APOC3 levels also reduced the odds of CAD (odds ratio, 0.90 per s.d. protein [95%CI,0.82–0.99]). Genetically lowered ANGPTL3 levels via common variants were not associated with CAD. However, meta-analysis of deleterious variants revealed that *ANGPTL3* inactivation protected against CAD (odds ratio, 0.79 per allele [95%CI, 0.69–0.90]). Analysis of lowered ANGPTL3, ANGPTL4, and APOC3 levels did not identify important safety concerns.

Conclusion: Human genetic evidence suggests that therapies aimed at reducing circulating levels of ANGPTL3, ANGPTL4, and APOC3 reduce the risk of CAD. ANGPTL4 lowering may also reduce the risk of T2D.

STRUCTURED GRAPHICAL ABSTRACT

Key Question: Does human genetics support that triglyceride-lowering drugs targeting ANGPTL3, ANGPTL4, and APOC3 will reduce the risk of cardiometabolic disease without causing side effects?

Key Finding: Genetically lowered circulating ANGPTL4 reduced coronary artery disease and type 2 diabetes risk. Genetically lowered ANGPTL3 and APOC3 also reduced coronary artery disease risk, but no impact on type 2 diabetes risk was observed.

Take-home Message: Human genetics suggest that ANGPTL3, ANGPTL4, and APOC3-lowering medications may prevent CAD. Medicines targeting ANGPTL4 may have added benefits for patients with type 2 diabetes.

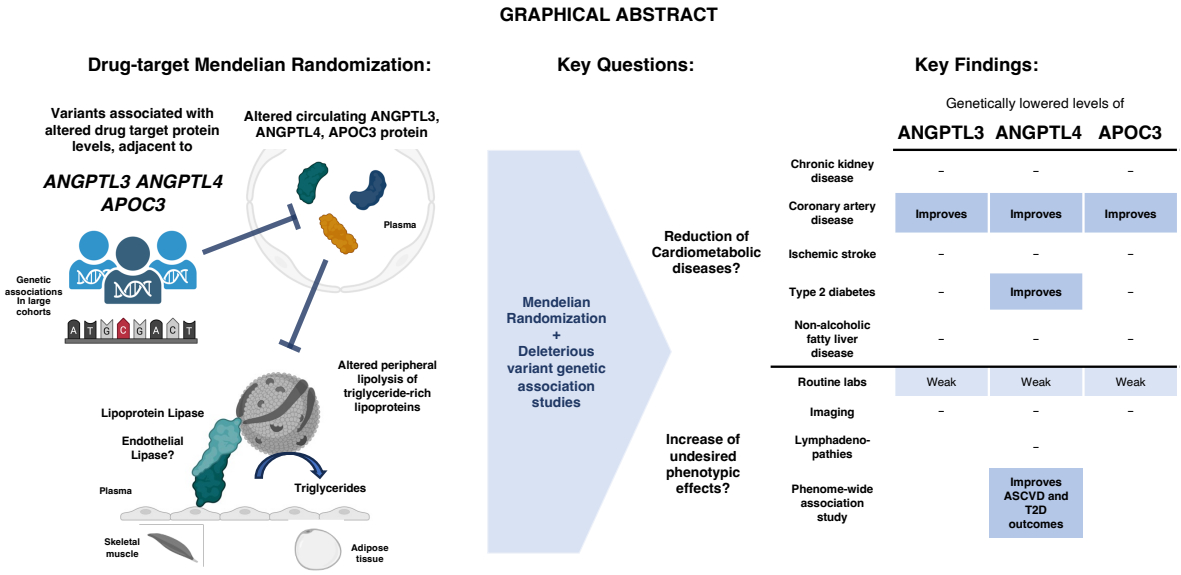

Graphical abstract summarizing the study's methods and findings.
Graphical abstract summarizing the overall study design. The 'Key Findings' figure provides a summary of the results categorized into three groups. The term 'improves' denotes a statistically significant association with a clinically relevant effect magnitude. The term 'weak' refers to a statistically significant association with no clinically significant effect. 'ASCVD' denotes atherosclerotic cardiovascular disease. 'T2D' denotes type 2 diabetes.

INTRODUCTION

APOC3, ANGPTL3, and ANGPTL4 are circulating proteins that regulate plasma cholesterol and triglyceride (TG) levels. They mainly act by inhibiting the enzyme lipoprotein lipase. All three proteins are actively pursued as pharmacological targets to treat dyslipidemia and reduce the risk of atherosclerotic cardiovascular disease. The inactivation of APOC3 using ASOs (Volanesorsen, Olezarsen) has been shown to substantially reduce plasma TG levels in different patient groups with severe hypertriglyceridemia (1). Volanesorsen is a second-generation ASO that was approved in Europe for treating familial chylomicronemia syndrome. Olezarsen is a third-generation ASO that very recently received fast-track designation from the FDA. Currently, several human trials are ongoing with an RNAi against APOC3 called ARO-APOC3.

Similar to APOC3, the inactivation of ANGPTL3 using monoclonal antibodies (Evinacumab) (2-6), antisense oligonucleotides (ASOs) (Vupanorsen) (7, 8), and RNAi (ARO-ANG3) has been shown to significantly lower plasma LDL-C and TG levels in various dyslipidemic patients groups (9). Evinacumab was approved in 2021 as a treatment for homozygous familial hypercholesterolemia (HoFH), while Vupanorsen was discontinued in 2021 due to the limited reduction in non-HDL-C and TG and increases in liver fat and enzymes (10). Recent case reports suggest that Evinacumab may promote the regression of atherosclerotic plaques in HoFH patients (11, 12).

Whereas the clinical development of anti-APOC3 and -ANGPTL3 treatments have progressed well, therapies targeting ANGPTL4 have faced delay because mice deficient in ANGPTL4 develop lethal mesenteric lymphadenopathy and chylous ascites when fed a diet high in saturated fatty acids (13-15). Whether whole-body inactivation of ANGPTL4 might trigger similar pathological features in humans is unclear. As an alternative pharmacological strategy, inactivating ANGPTL4 specifically in the liver holds considerable promise (16). Despite these challenges, targeting ANGPTL4 presents a promising opportunity, as it may not only lower triglycerides and remnant cholesterol but also redirect lipids away from ectopic sites and towards adipose tissue, potentially protecting against type 2 diabetes (17).

Human genetic data can be leveraged to predict the clinical effect of the pharmacological inactivation of genes or proteins. Here, we aimed to compare the predicted therapeutic effects of APOC3, ANGPTL3, and ANGPTL4 inactivation by investigating the biological and clinical impact of inactivation variants in the respective genes. In addition, to address safety concerns, we compared the predicted detrimental effects of APOC3, ANGPTL3, and ANGPTL4 inactivation on relevant disease outcomes. We conclude that therapies specifically aimed at decreasing plasma ANGPTL3, ANGPTL4, and APOC3 levels are expected to reduce the risk of coronary artery disease without raising safety concerns. Therapies targeting ANGPTL4 levels are expected to favorably impact the risk of type 2 diabetes. This suggests that reducing ANGPTL4 could offer therapeutic advantages to a wider group of patients with dyslipidemia and type 2 diabetes.

90 **METHODS**

91 **Study design**

92 The study was performed in four sequential steps as summarized in **Figure 1**. First, a two-sample
93 Mendelian randomization (MR) study was conducted to measure the association between ANGPTL3,
94 ANGPTL4, and APOC3 lowering with cardiometabolic diseases and risk factors. Second, two-sample
95 MR was conducted to measure the target proteins' association with phenotypes related to potential
96 adverse effects. Third, validation analyses were conducted to further assess the plausibility of the
97 findings obtained from steps 1-2. Lastly, to measure the association between profound genetic
98 inactivation of the target proteins and CAD, deleterious variant analyses in the UK Biobank were
99 performed and meta-analysed with previous studies.

100 **Steps 1-2**

101 **Genetic instruments**

102 To estimate the causal effects of pharmacologically inactivating the *ANGPTL3*, *ANGPTL4*, and
103 *APOC3* genes, we performed two-sample drug-target MR. We used, as instrumental variables (IV),
104 genetic variants within 2.5 kilobase pairs (Kb) of the target gene that had genome-wide significant
105 associations (P-value $\leq 5\times10^{-8}$) with protein abundance (called *cis* protein quantitative trait loci, *cis*-
106 pQTLs) or plasma TG, as determined by genome-wide association studies (GWAS). Variants
107 adjacent to the target genes were clumped at an LD threshold of $r^2 \geq 0.10$ to avoid GLS-related
108 multicollinearity issues. Residual LD was accounted for using the generalized least squares (GLS)
109 IVW estimator described below.

110

111 **Drug-target MR**

112 The precision of the inverse-variance weighted (IVW) estimator can be influenced by LD-related
113 correlation between the genetic IV in the drug target genes *cis'* position. Therefore, we used a GLS IVW
114 MR estimator to correct for this potential source of bias (18, 19). The GLS-corrected MR approach can
115 be conceptualized as combining the independent information of variants near a target gene while
116 maintaining robust standard errors through weighting for their LD-related correlation. Further
117 information regarding Drug-target MR methodology, GLS, LD matrix sensitivity, and sample overlap
118 bias are found in the **Supplemental Methods**.

119 Due to the complex structure of the *APOA1-APOA5-APOC3* locus, we supplemented the original
120 analyses with a second model of APOC3 lowering. In this model, APOC3 lowering was instrumented
121 through the *APOC3 c.55+1G>A* splice donor loss variant solely, as this variant is a high-confidence
122 predicted loss-of-function variant (gnomAD Genome Aggregation Database v.4.0.0,
123 https://gnomad.broadinstitute.org) independent of other common variants in this genomic region (20).
124 The *APOC3 c.55+1G>A* MRs used a Wald ratio estimator. Furthermore, we used *LPL*-adjacent and
125 genome-wide TG-associated variants as positive controls. LPL was analyzed using drug-target MR. For

126 the genome-wide TG-associated variant MR, we tested the causal effect of TG using variants in
127 chromosomes 1-22 associated with TG at P-value $\leq 5\times10^{-8}$. An LD clumping window of 500 Kb and a
128 threshold of $r^2 \geq 0.001$ was applied before analysis using an IVW estimator.

129 **Data sources**

130 Plasma protein abundance was measured in GWAS using the SomaScan and Olink platforms (21, 22).
131 GWAS data on plasma TG, LDL cholesterol, HDL cholesterol, apolipoprotein B, apolipoprotein A1,
132 and lipoprotein(a) were retrieved from the 2018 Neale Lab UK biobank analysis
133 (http://www.nealelab.is/uk-biobank/). For the functional variant analyses, genetic association data on
134 TG, LDL cholesterol, and HDL cholesterol were retrieved from the AstraZeneca UK biobank exome
135 sequencing-based phenome-wide association study (PheWAS) portal (23). We obtained outcome
136 summary data from GWAS of six cardiometabolic disease endpoints, 16 cardiometabolic risk markers,
137 43 routine clinical chemistry tests, 11 internal organ MRI measurements, and five abdominal
138 lymphadenopathy-related phenotypes (see **Table 1**, **Supplemental Table 1,** and **Supplemental**
139 **Methods**). Phenome-wide MR analyses were conducted in FinnGen and the UK biobank. FinnGen
140 integrates genotype data from Finnish biobanks with longitudinal health registry data (24). The UK
141 Biobank is a large-scale research resource containing genetic, blood chemistry, imaging, and health
142 record data from half a million UK participants (25). The FinnGen data freeze 10 and UK biobank meta-
143 analysis (https://public-metaresults-fg-ukbb.finngen.fi) stores genetic association statistics on 694
144 disease-related outcomes from 301,552–882,347 individuals. Further details on the selection of GWAS
145 and the definition of exposures and outcomes are given in the **Supplemental Methods**.

146 **Colocalization analyses**

147 Drug-target MR substantially relies on the assumption that LD (a phenomenon in which neighboring
148 genetic variants are inherited together more frequently than anticipated by chance (26)) does not
149 confound the association between variant and outcome. In cases where there are distinct genetic variants
150 affecting both the exposure and the outcome, and they are connected through LD, there is a risk of
151 making incorrect conclusions (27). To limit this issue, we performed colocalization analyses, which test
152 whether two independent association signals in the same gene region are consistent with having a single
153 shared causal variant (that is, testing if the association signals are 'colocalized') (28). To assess possible
154 confounding from LD, all drug target MR analyses were complemented by colocalization analysis of
155 the 500 Kb (±250 Kb) region surrounding each target gene (28). Further details regarding the
156 colocalization analyses are provided in the **Supplemental Methods**.
157

158 **Lymphadenopathy and phenome-wide MR analyses**

159 A Wald ratio estimator was used for the single-variant MR of lymphadenopathy-related phenotypes and
160 the phenome-wide MR conducted in FinnGen (29). The variants were selected based on being within

161 2.5 Kb of the drug target gene, their strength of association with target protein plasma abundance ($P \leq$
162 5×10^{-8}), their strength of association with triglyceride levels ($P \leq 5\times10^{-8}$), availability, and their
163 functional consequence. For further details regarding genetic instrument justification for the phenome-
164 wide MRs, see the **Supplemental Methods**.

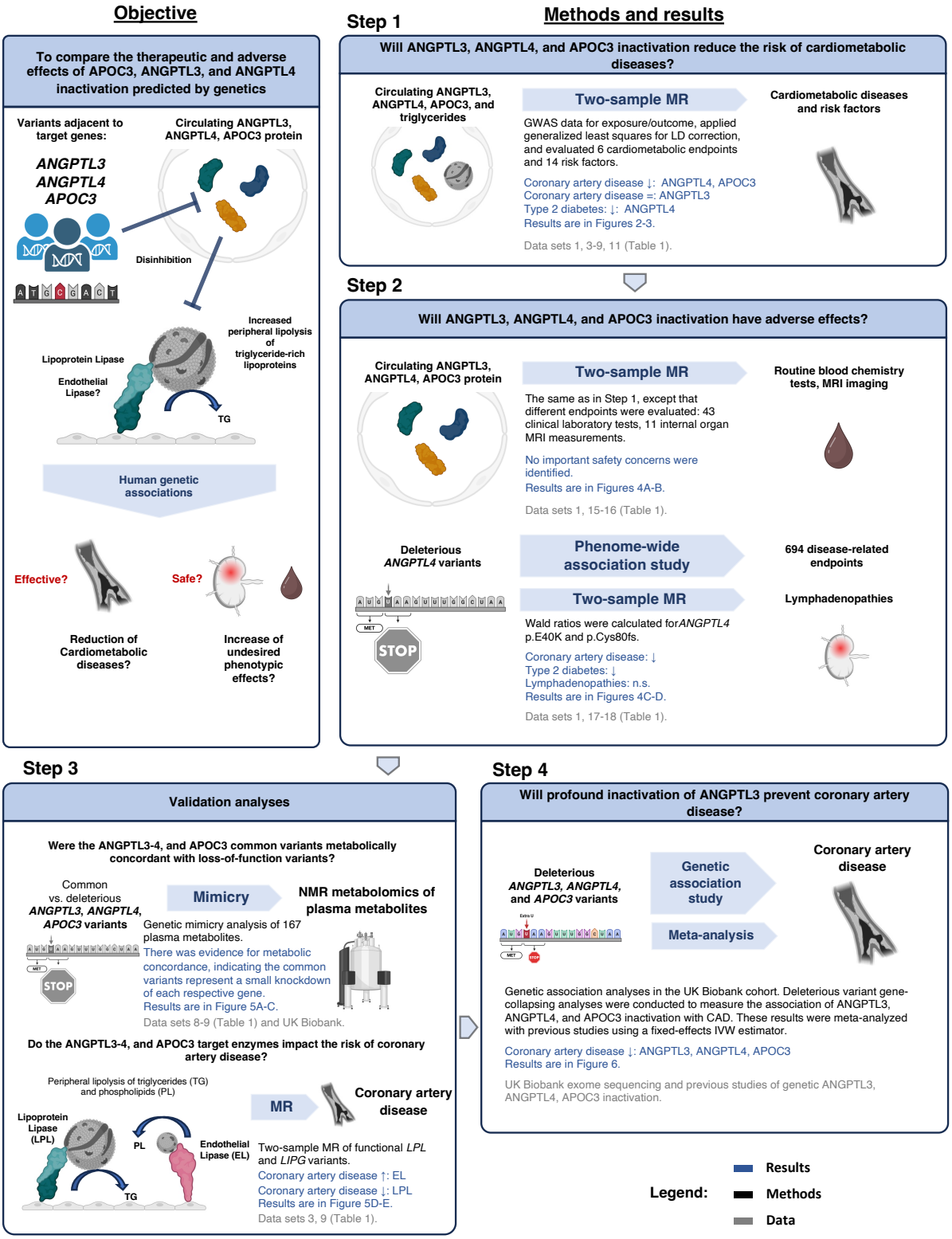

Figure 1. Study design flow chart summarizing the objective, methods, and results.
'LD' indicates linkage disequilibrium. 'n.s.' denotes not significant. 'LPL' indicates lipoprotein lipase. 'MR' indicates Mendelian Randomization. 'EL' indicates endothelial lipase. 'CAD' indicates coronary artery disease. 'IVW' indicates inverse-variance weighted.

170

Table 1. Description of GWAS data sets

	No	Trait	First author (year)	Consortium	Sample size (events/total)	Population
pQTL	1	Plasma protein abundance (SomaScan)	Ferkingstad (2021) (21)	deCODE	35,559	Icelandic
	2	Plasma protein abundance (Olink)	Dhindsa (2023) (22)	Not available	50,829	British
Diseases	3	Coronary artery disease	Aragam (2022) (30)	CARDioGRAMplusC4D; EPIC-CVD	181,522 / 1,165,690	European
	4	Chronic kidney disease	Wuttke (2019) (31)	CKDGen	41,395 / 480,698	European
	5	Ischemic stroke	Mishra (2022) (32)	GIGASTROKE	62,100 / 1,296,908	European
	6	Non-alcoholic fatty liver disease	Ghodsian (2021) (33)	Not available	8,434 / 787,048	European
	7	Type 2 diabetes	Mahajan (2018) (34)	DIAGRAM	74,124 / 898,130	European
Risk factors	8	Plasma total, HDL, and LDL cholesterol; Apolipoprotein B; Apolipoprotein A1; TG; Lipoprotein(a); HbA1c	Neale lab (2018)	Not available	273,896 – 344,278;	British
	9	HDL, and LDL cholesterol; TG; NMR metabolomics	Wang (2021) (23); Nag (2023) (35)	AZPheWAS	95,077 – 376,311	British
	10	NMR metabolomics, including total lipoprotein phospholipids	Elsworth (2020) (36)	MRC-IEU	110,058 – 115,078	British
	11	Systolic blood pressure; diastolic blood pressure	Evangelou (2018) (37)	Not available	757,601	European
	12	Body mass index; waist-hip ratio	Pulit (2018) (38)	GIANT	694,649 – 806,834	European
	13	Body fat percentage; NMR total triglycerides; NMR total phospholipids	Elsworth (2020) (36)	MRC-IEU	115,078 – 454,633	British
	14	Plasma creatinine estimated glomerular filtration rate (eGFR); cystatin C eGFR	Stanzick (2021) (39)	CKDGen	1,004,040; 1,201,909	European; 86% European
Safety-related	15	Magnetic resonance imaging of internal organs	Liu (2021) (40)	Not available	25,617 – 32,860	British
	16	Routine blood chemistry tests	Neale lab (2018)	Not available	30,565 – 350,812	British
	17	Acute lymphadenitis; Acute peritonitis; Ascites; Intestinal malabsorption; Non-infectious lymphatic disorders	Neale lab (2018); Kurki (2023) (24)	Not available; FinnGen	620 – 4,982 / 270,172 – 382,633; 798 – 1643 / 295,812 – 341,350	British; Finnish
	18	Phenome-wide association study	FinnGen (2023) (24)	Pan-UK Biobank + FinnGen meta-analysis	110 – 279,543 / 301,552 – 882,347	British; Finnish

171 'NMR' indicates nuclear magnetic resonance spectroscopy.

172 **Step 3**

173 **Genetic mimicry analyses**

174 Genetic mimicry analysis was used to compare the metabolic concordance between common and
175 deleterious variants adjacent to the *ANGPTL3*, *ANGPTL4*, and *APOC3* genes. This method uses linear
176 regression to determine the extent of similarity between different variants' genetic associations in high-
177 dimensional data sets (41, 42). The degree of concordance was reported as the coefficient of
178 determination (R^2). Genetic associations between the common variants and 167 plasma metabolites were
179 measured by drug-target MR with plasma TGs as the exposure using data sets 8 and 10 (see **Table 1**).
180 Deleterious variants were defined as any protein-truncating variant with an allele frequency <0.05 or
181 missense variants with a REVEL pathogenicity prediction score >0.25 and allele frequency <0.00025
182 (see **Supplemental methods**). The effects of deleterious variants were determined by regressing plasma
183 concentration of metabolites on deleterious variant carrier status in 181,672 UK Biobank participants
184 (see **Supplemental Methods** for details).

185

186 **Robustness checks and sensitivity analyses**

187 We performed sensitivity MR analyses of *ANGPTL3*, *ANGPTL4*, *APOC3*, *LPL*, and *LIPG* on CAD by
188 restricting the genetic instrument selection to variants within these target genes predicted to have
189 functional impacts. This strategy aimed to mitigate potential biases arising from common non-coding
190 small-effect variants outside the target genes, which could be confounded due to linkage disequilibrium
191 with other genes in the same genomic region. Ensembl Variant Effect Predictor (VEP) version 109 (43)
192 was used to annotate variants within 2.5 Kb of the target gene associated ($P \leq 0.01$) with target protein
193 levels and plasma triglycerides. Non-coding variants outside of the 5' untranslated region (UTR), 3'
194 UTR, or splice site regions were filtered out and excluded from further analysis, as were missense
195 variants lacking SIFT deleterious or PolyPhen likely or probably damaging annotations. MR was
196 conducted for single variants using the Wald ratio estimator, and meta-analysis was performed using a
197 random-effects IVW estimator.

198 **Step 4**

199 **Meta-analysis of the impact of deleterious variants on CAD**

200 We conducted genetic association analyses in the UK Biobank (see **Supplemental Methods**) and meta-
201 analyzed the results with previous studies to assess how deleterious variants in *ANGPTL3*, *ANGPTL4*,
202 and *APOC3* impact CAD risk. To minimize the influence of incorrect genotype calls for rare variants,
203 the meta-analysis was limited to studies where genotypes were determined by DNA sequencing. When
204 multiple papers reported on individuals from overlapping cohorts or case-control studies, we selected
205 the substudy with the largest sample size for inclusion in the meta-analysis. The meta-analyses were
206 restricted to European ancestries. We determined the impact of the inactivating variants on CAD risk
207 per mmol/L reduction of TG and per inactivating allele using fixed-effect IVW estimators. If no within-

208 sample association of inactivating variants with TG concentrations (in mmol/L) was available, the
209 combined IVW meta-analysis TG estimate was used as the denominator to determine the CAD odds per
210 mmol/L TG effect. Statistical heterogeneity across studies was estimated by calculating the Cochran Q
211 statistic.
212
213 **Statistics**
214 **Multiple testing**
215 P-values and 95% confidence intervals (CI) are reported using analysis-type Bonferroni multiple
216 comparisons correction. In the primary MR analyses, we corrected for the five cardiometabolic disease
217 outcomes that were run across three different drug-target gene exposures (*ANGPTL3, ANGPTL4,*
218 *APOC3*) for protein abundance, and four genes for the TG exposure (*ANGPTL3, ANGPTL4, APOC3,*
219 *LPL*). Additionally, we included five genome-wide triglyceride MR models, totaling 40 comparisons
220 for the cardiometabolic disease outcomes. In the cardiometabolic risk factor MR analyses of *cis*-pQTLs,
221 we made corrections for 45 multiple comparisons (15×3). Similarly, imaging and blood chemistry MR
222 analyses were corrected for 33 (11×3), and 129 (43×3) multiple comparisons, respectively. We did not
223 perform multiple comparison corrections for the *ANGPTL4*-targeted MR analyses of the
224 lymphadenopathy-related phenotypes. This was because identifying potential safety concerns that
225 needed to be addressed was considered more critical than stringent multiplicity correction for these
226 specific outcomes. Similarly, the primary motivation for performing the functional variant-limited CAD
227 MR analyses and deleterious variant meta-analysis was to reduce the risk of false-negative findings.
228 Additionally, we wanted to ensure that these CIs and P-values remained comparable across different
229 studies. These CIs and P-values were, therefore, not corrected for multiple comparisons. The
230 significance threshold in the phenome-wide *cis*-pQTL MR analyses was set at 2082 multiple
231 comparisons (694 phenotypes in the FinnGen R10 and UK biobank meta-analysis, times three genes).

232 **RESULTS**

233 The results of the drug-target MR analyses of cardiometabolic diseases, cardiometabolic risk factors,
234 and the safety-related endpoints are presented in **Figure 2**, **Figure 3**, and **Figure 4**, respectively. MR
235 scatter, colocalization plots, and results tables with greater detail are provided in **Supplemental Figures**
236 **1-2** and **Supplemental Table 2**. Detailed PheWAS results are provided in **Supplemental Tables 6-9**.
237 The genetic variants selected for inclusion as instrumental variables in one or more of the MR analyses
238 are shown in **Table 2**.

Table 2. Genetic instruments

	rsID	Variant	HGVS	Consequence	Frequency	Effect (P-value) Protein (SomaScan)	Protein (Olink)	Protein (ELISA)‡	TG
ANGPTL3	rs79151558	1:62595131:A>G		Upstream variant	0.028	-0.32 (8.1e-39)	-0.27 (1.4e-36)	-	-0.06 (5.4e-13)
	rs11207997*	1:62596235:C>T		Upstream variant	0.338	-0.22 (1.2e-144)*	-0.31 (<2e-308)*	-	-0.08 (2.7e-221)*
	rs17123728	1:62602628:G>A	c.931+248G>A	Intron variant	0.04	n.s.	-	-	0.03 (2.5e-08)
	rs35285100	1:62603486:T>C	c.932-483T>C	Intron variant	0.071	0.10 (2.3e-09)	0.08 (6.3e-10)	-	n.s.
	rs10789117*	1:62606594:A>C		Downstream variant	0.354	-0.22 (1.7e-144)*	-0.31 (<2e-308)*	-	-0.08 (1.6e-221)*
	rs6678483*	1:62608771:C>A		Downstream variant	0.354	-0.22 (1.7e-144)*	-0.31 (<2e-308)*	-	-0.08 (2e-221)*
ANGPTL4	rs116843064‡	19:8364439:G>A	p.Glu40Lys‡	Missense variant‡	0.024	-0.32 (6.6e-35)	-0.35 (6.8e-48)	-0.45 (4.8e-05)‡	-0.21 (3.2e-127)
	rs149480839	19:8368237:C>T	c.548-982C>T	Intron variant	0.03	n.s.	-	-	-0.05 (2.6e-14)
	rs139469000	19:8376253:C>T		Downstream variant	0.28	n.s.	-	-	-0.02 (1.7e-09)
APOC3	rs2727788	11:116828247:C>A		Upstream variant	0.262	n.s.	-	-	-0.05 (7.3e-83)
	rs138326449	11:116830638:G>A	c.55+1G>A	Splice donor variant	0.002	-2.19 (3.2e-142)	-	-	-0.86 (3.4e-157)
	rs5141†	11:116831407:T>C	c.179+511T>C	Intron variant	0.916	-0.17 (2.1e-38)†	-	-	-0.19 (<2e-308)†
	rs5132	11:116832062:C>T	c.180-702C>A	Intron variant	0.015	n.s.	-	-	0.06 (3.1e-08)
	rs12721031	11:116833789:C>T		Downstream variant	0.023	n.s.	-	-	-0.06 (2.6e-12)
	rs10750098†	11:116834852:G>T		Downstream variant	0.115	-0.17 (2.1e-38)†	-	-	-0.19 (<2e-308)†
	rs12721028	11:116834874:A>G		Downstream variant	0.159	n.s.	-	-	0.04 (2e-35)
	rs12718462	11:116835003:T>C		Downstream variant	0.066	n.s.	-	-	-0.05 (1.8e-22)

Showing the genetic variants selected for inclusion as instrumental variables in one or more of the MR analyses whose results are shown in **Figures 2-4**. The specific instruments used in each separate MR analysis are provided in **Supplemental Table 2**. *Cis*-pQTLs meeting the significance threshold (P-value ≤ 5×10^{-8}) were initially identified in the SomaScan protein GWAS. These cis-pQTLs were then cross-referenced with the UK Biobank Olink protein GWAS to determine if the effect estimates were consistent. Variant consequences were retrieved from the Ensembl Variant Effect Predictor (version 109) (43). 'Effect' indicates the 1 s.d. protein abundance (retrieved from (21, 22)) or mmol/L TG change (retrieved from http://www.nealelab.is/uk-biobank/) per allele. 'rsID' denotes Reference single nucleotide polymorphism ID. 'HGSV' indicates Human Genome Structural Variation Consortium nomenclature for sequence variants. 'n.s.' indicates not significant.

*† These variants were in strong linkage disequilibrium (LD) and, therefore, showed the same associations with TG levels and plasma ANGPTL3/APOC3 abundance. Because they were in strong LD, they were never included in the same MR model (see **Methods** and **Supplemental Table 2**).

‡ The association between *ANGPTL4* p.E40K coding variant carrier status and plasma ANGPTL4 protein was confirmed in a separate study by ELISA using antibodies that were shown by Western blotting to similarly detect wildtype ANGPTL4 and ANGPTL4 containing the E40K substitution, indicating that the association was not attributable to epitope-binding artifacts (see **Supplemental Methods**).

254 **Step 1**

255 **Drug-target MR of cardiometabolic diseases**

256 Genetically mediated changes in plasma ANGPTL3 protein abundance were not associated with a
257 reduced risk of any cardiometabolic outcome (**Figure 2A**), nor were *ANGPTL3*-mediated changes in
258 plasma TG (**Figure 2B**).

259 The p.E40K coding variant was the only variant that qualified as a *cis*-pQTL in the *ANGPTL4* region.
260 *ANGPTL4* p.E40K is a common missense variant (allele freq. ~2% in Europeans) that destabilizes
261 ANGPTL4 after secretion and prevents ANGPTL4 from inhibiting LPL (44). The association between
262 the *ANGPTL4* p.E40K coding variant and plasma ANGPTL4 protein was validated via ELISA in a
263 separate cohort. The association was -0.45 s.d. protein per allele, $P=4.8\times10^{-5}$, comparable to the
264 associations detected with the Olink and Somascan platforms (see **Table 2**). The ELISA antibodies
265 detected wild-type and E40K ANGPTL4 proteins to a comparable degree, as determined by Western
266 blot analysis (see **Supplemental Methods** for details). This suggests that the observed association was
267 not attributable to epitope-binding artifacts.

268 Changes in ANGPTL4 protein levels via *ANGPTL4* p.E40K were associated with a decreased risk of
269 CAD (OR: 0.57, $P=1\times10^{-19}$), and T2D (OR: 0.73, P=0.001) (**Figure 2A**). Similarly, changes in plasma
270 TG levels via three *ANGPTL4*-adjacent variants were associated with a decreased risk of CAD (OR:
271 0.43, $P=1\times10^{-21}$), and T2D (OR: 0.62, $P=4\times10^{-4}$) (**Figure 2B**). In addition, colocalization analyses
272 indicated a high probability of *ANGPTL4* p.E40K being a shared causal variant for ANGPTL4 levels
273 and TG levels with CAD and T2D (pp.H_4: 98–100%) (**Figures 2A-B**).

274 Changes in APOC3 levels caused by *APOC3*-adjacent variants were associated with a reduced risk of
275 CAD (OR: 0.90, P=0.009) (**Figure 2A**), as were changes in TG levels through *APOC3*-adjacent variants
276 (OR: 0.80, $P=4\times10^{-11}$). The *APOC3* c.55+1G>A splice donor loss variant had a substantial impact on
277 plasma APOC3 levels (-2.19 s.d. protein, $P=3.2\times10^{-142}$) and plasma TG (-0.86 mmol/L, $P=3.4\times10^{-157}$)
278 (**Table 2**). When compared to the model allowing for multiple variants in the *APOC3* region, APOC3
279 lowering modeled through the *APOC3* c.55+1G>A variant demonstrated a comparable correlation with
280 CAD in terms of the direction of its effect. However, the association was non-significant (**Figure 2**).

281 Similar to APOC3 and ANGPTL4, changes in plasma TG levels through *LPL*-adjacent variants were
282 associated with a reduced risk of CAD (OR: 0.69, $P=1\times10^{-24}$), NAFLD (OR: 0.66, P=0.021), and T2D
283 (OR: 0.73, $P=6\times10^{-10}$) (**Figure 2B**).

284

Cardiometabolic diseases

A. Exposure: Target protein abundance

Outcome	Events/Total	No. SNPs		Odds ratio (95% CI)	P-value	Coloc.
Coronary artery disease	181,522 / 1,165,690	*ANGPTL3*	3	0.98 (0.91;1.06)	1.00	H1: 93%
		ANGPTL4	1	0.57 (0.47;0.69)	1e−19	H4: 100%
		APOC3	2	0.90 (0.83;0.99)	0.009	H3: 100%
		APOC3 c.55+1G>A	1	0.94 (0.84;1.04)	1.00	
Chronic kidney disease	41,395 / 480,698	*ANGPTL3*	3	0.97 (0.84;1.12)	1.00	H1: 94%
		ANGPTL4	1	0.99 (0.68;1.44)	1.00	H1: 94%
		APOC3	1	0.86 (0.63;1.17)	1.00	H1: 95%
		APOC3 c.55+1G>A	0			
Ischemic stroke	62,100 / 1,296,908	*ANGPTL3*	3	1.08 (0.97;1.21)	0.66	H1: 95%
		ANGPTL4	1	0.78 (0.57;1.08)	0.54	H1: 74%
		APOC3	1	0.97 (0.77;1.23)	1.00	H1: 94%
		APOC3 c.55+1G>A	0			
Non−alcoholic fatty liver disease	8,434 / 787,048	*ANGPTL3*	3	1.05 (0.82;1.36)	1.00	H1: 97%
		ANGPTL4	1	1.07 (0.61;1.87)	1.00	H1: 93%
		APOC3	1	0.91 (0.55;1.53)	1.00	H1: 94%
		APOC3 c.55+1G>A	0			
Type 2 diabetes	74,124 / 898,130	*ANGPTL3*	3	1.00 (0.91;1.11)	1.00	H1: 90%
		ANGPTL4	1	0.73 (0.58;0.93)	0.001	H4: 98%
		APOC3	2	1.00 (0.90;1.11)	1.00	H3: 57%
		APOC3 c.55+1G>A	1	1.08 (0.95;1.21)	1.00	

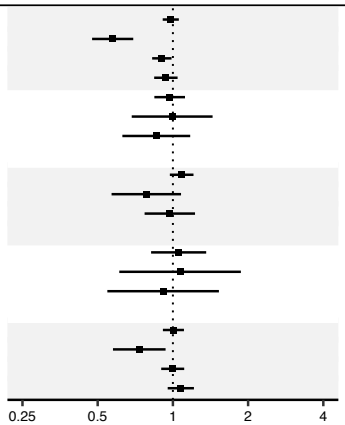

Odds ratio per s.d. lowered protein abundance (95% CI)

B. Exposure: Triglycerides

Coronary artery disease	181,522 / 1,165,690	*ANGPTL3*	3	0.96 (0.78;1.18)	1.00	H1: 96%
		ANGPTL4	3	0.43 (0.33;0.57)	1e−21	H4: 100%
		APOC3	7	0.80 (0.72;0.89)	4e−11	H4: 100%
		APOC3 c.55+1G>A	1	0.85 (0.65;1.12)	1.00	
		LPL	20	0.69 (0.61;0.77)	1e−24	H3: 100%
		Genome−wide TG QTLs	117	0.76 (0.69;0.84)	8e−19	
Chronic kidney disease	41,395 / 480,698	*ANGPTL3*	3	0.85 (0.57;1.27)	1.00	H1: 94%
		ANGPTL4	3	0.97 (0.57;1.67)	1.00	H1: 94%
		APOC3	6	0.85 (0.68;1.05)	0.53	H1: 95%
		APOC3 c.55+1G>A	0			
		LPL	19	0.92 (0.74;1.14)	1.00	H1: 94%
		Genome−wide TG QTLs	95	1.00 (0.88;1.13)	1.00	
Ischemic stroke	62,100 / 1,296,908	*ANGPTL3*	3	1.21 (0.89;1.63)	1.00	H1: 94%
		ANGPTL4	3	0.74 (0.47;1.17)	1.00	H1: 74%
		APOC3	6	0.99 (0.85;1.16)	1.00	H1: 95%
		APOC3 c.55+1G>A	0			
		LPL	14	0.97 (0.82;1.15)	1.00	H1: 96%
		Genome−wide TG QTLs	89	0.98 (0.90;1.07)	1.00	
Non−alcoholic fatty liver disease	8,434 / 787,048	*ANGPTL3*	3	1.14 (0.56;2.31)	1.00	H1: 97%
		ANGPTL4	3	1.05 (0.46;2.39)	1.00	H1: 93%
		APOC3	5	0.96 (0.68;1.37)	1.00	H1: 95%
		APOC3 c.55+1G>A	0			
		LPL	14	0.66 (0.44;0.97)	0.021	H3: 52%
		Genome−wide TG QTLs	83	0.92 (0.68;1.23)	1.00	
Type 2 diabetes	74,124 / 898,130	*ANGPTL3*	3	1.01 (0.77;1.32)	1.00	H1: 95%
		ANGPTL4	3	0.62 (0.44;0.88)	4e−04	H4: 98%
		APOC3	7	0.89 (0.78;1.01)	0.11	H3: 58%
		APOC3 c.55+1G>A	1	1.20 (0.89;1.63)	1.00	
		LPL	19	0.73 (0.63;0.85)	6e−10	H3: 51%
		Genome−wide TG QTLs	104	0.87 (0.70;1.08)	1.00	

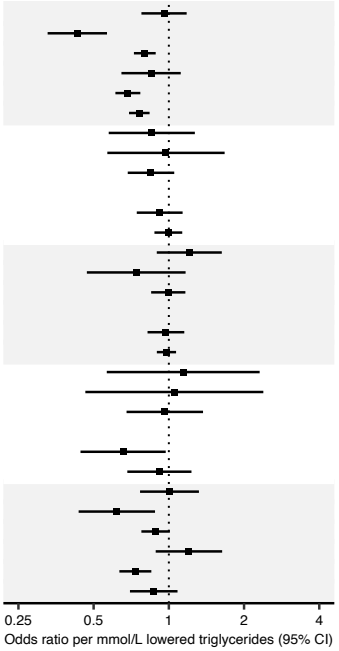

Odds ratio per mmol/L lowered triglycerides (95% CI)

Figure 2. Results of MR analyses of cardiometabolic disease outcomes.

A: Forest plot and table of the *cis*-pQTL-based MR analyses. 'Events/total' indicates the outcome study's case count and total sample size. 'No. SNPs' specifies the number of variants included in the MR model. Zero SNPs indicate that none of the genetic instruments were detected in the outcome data set. 'Coloc.' shows the colocalization hypothesis ($H_{0\text{-}4}$) with the highest posterior probability (see the 'Methods' section for details about their interpretation). **B:** Results of the MR analysis using TG levels as the exposure. The 'Genome-wide TG QTLs' and 'LPL' models were positive controls. 'Genome-wide TG QTLs' indicate the MR model that included independent ($r^2 < 0.001$, 500Kb clumping window) variants associated with TG levels ($P \leq 5\times10^{-8}$) across chromosomes 1-22. 'LPL' denotes lipoprotein lipase.

Drug-target *cis*-pQTL MR of cardiometabolic risk factors

Genetically lowered plasma ANGPTL3 levels were associated with reduced total cholesterol (-0.27 mmol/L, $P=2\times10^{-107}$), TG (-0.34 mmol/L, $P=6\times10^{-206}$), LDL-C (-0.15 mmol/L, $P=2\times10^{-57}$), ApoB (-0.03 g/, $P=3\times10^{-36}$), and ApoA-I levels (-0.05 g/L, $P=1\times10^{-51}$), while the effect on HDL-C was comparatively weak (-0.02 mmol/L, $P=4\times10^{-5}$) (**Figure 3**).

Genetically lowered plasma ANGPTL4 levels instrumented through the p.E40K variant were associated with reduced plasma TG (-0.65 mmol/L, $P=1\times10^{-125}$) and weakly reduced ApoB levels (-0.02 g/L, P=0.038), as well as increased ApoA1 (0.11 g/L, $P=1\times10^{-55}$) and HDL-C levels (0.24 mmol/L, $P=7\times10^{-134}$) (**Figure 3**). Genetically lowered plasma ANGPTL4 levels were also associated with modest reductions in the waist-hip ratio (-0.09 s.d., P=0.004), and a small increase in body fat percentage (0.07 s.d., P=0.008) (**Figure 3**).

Genetically lowered plasma APOC3 levels were associated with reduced TG levels (-0.58 mmol/L, $P < 2\times10^{-308}$) (**Figure 3**). APOC3 levels were also associated with ApoB (-0.03 g/L, $P=1\times10^{-22}$), LDL-C (-0.10 mmol/L, $P=6\times10^{-18}$), HDL-C (0.16 mmol/L, $P = 2\times10^{-238}$), and total cholesterol (-0.08 mmol/L, $P=5\times10^{-6}$) (**Figure 3**). In terms of association and effect directionality, these results closely resembled those of the *APOC3 c.55+1G>A* model (**Figure 3**).

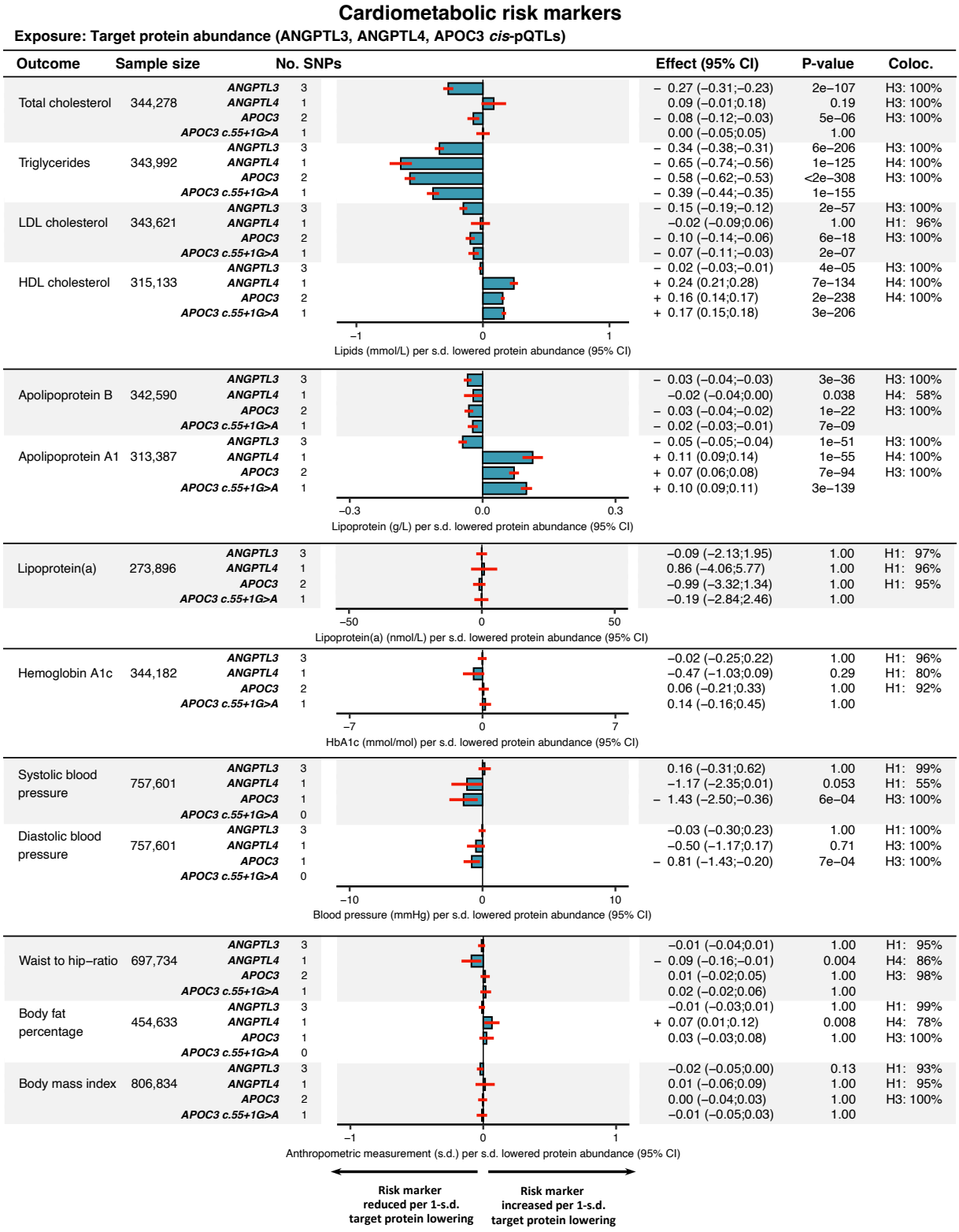

Figure 3. Results of MR analyses of cardiometabolic disease risk factors.
The results are presented as bar plots, showing the magnitude of the effect per s.d. lowered protein abundance. The red lines indicate the 95 % CI. The results from cis-pQTL MR of the estimated glomerular filtration rate (eGFR) by Cystatin C and plasma Creatinine, respectively, are given in **Supplemental Figure 3**.

315 **Step 2**

316 **Drug-target MR of potential adverse effects**

317 Genetic lowering of plasma protein levels of the target genes was not associated with any of the MRI
318 imaging endpoints (**Figure 4A**). 9, 3, 9, and 6 out of the 43 routine clinical laboratory tests showed
319 statistically significant associations by drug-target cis-pQTL MR of the ANGPTL3, ANGPTL4,
320 APOC3, and c.55+1G>A models, respectively (**Figure 4B**). The effect magnitudes were weak. For
321 example, genetically lowered ANGPTL3 and APOC3 levels were significantly associated with
322 increased platelet count. However, the effect was estimated to be 4–5×10^9 cells/L (equalling 0.06-0.08
323 s.d.) per s.d. lowered plasma protein levels, which was minimal compared to the population mean value
324 of 252×10^9 cells/L.

325 Given that safety concerns have arisen from preclinical models of ANGPTL4 deficiency, we conducted
326 targeted cis-pQTL MR analyses of ANGPTL4 on disease phenotypes that may be associated with
327 abdominal lymphadenopathy. The mechanism behind the fatal chylous lymphadenopathy observed in
328 mice was purportedly the loss of inhibition of LPL in macrophages, which caused them to take up excess
329 lipids, leading to massive inflammation in the mesenteric lymph system (14). Exposure to ANGPTL4
330 inactivation was instrumented using two different models: by the *ANGPTL4* p.E40K coding variant, and
331 by the *ANGPTL4* p.Cys80frameshift (fs) variant. *ANGPTL4* p.Cys80fs is a high-confidence predicted
332 loss-of-function variant (gnomAD v.4.0.0). It is enriched in Finns compared to non-Finnish Europeans
333 (allele frequency: 0.63% vs. 0.05%). *Cis*-pQTL MR via the relatively common *ANGPTL4* p.E40K
334 variant was conducted at five different phenotypes that may be related to lymphadenopathy and
335 malabsorptive states. Four had overlapping phenotype codes between the UK biobank and FinnGen and
336 were meta-analyzed using IVW meta-analysis. ANGPTL4 levels via p.E40K were not associated with
337 any of the five phenotypes (**Figure 4C**). However, since the confidence intervals were wide, we cannot
338 fully exclude an association of p.E40K within this interval. Genetically lowered plasma ANGPTL4
339 levels via the *ANGPTL4* p.Cys80fs variant were not associated with any of the four FinnGen phenotypes
340 that may be related to lymphadenopathy and malabsorptive states (**Figure 4C**).

341 To investigate if there was any genetic evidence for unknown ANGPTL4-mediated side effects, we
342 performed cis-pQTL MR on 694 disease-related phenotypes in FinnGen and the UK Biobank via the
343 *ANGPTL4* p.E40K and p.Cys80fs variants. Using a phenome-wide significance threshold of $P \leq \frac{0.05}{3\times694}$,
344 we found no evidence for increased risk of any endpoint via p.E40K- or p.Cys80fs-lowered ANGPTL4
345 levels (**Figure 4D**). Instead, we found phenome-wide evidence that p.E40K reduced the risk of four
346 CAD-related phenotypes, including myocardial infarction and one T2D-related phenotype, while also
347 being associated with a lowered probability of statin prescription, lipoprotein disorders, and
348 hypercholesterolemia (**Figure 4D**). Additionally, *ANGPTL4* p.Cys80fs was associated with a decreased
349 risk of two T2D-related outcomes and a lowered probability of statin prescription and
350 hypercholesterolemia diagnosis (**Figure 4D**).

351 The phenome-wide MR results of lowered plasma ANGPTL4 levels were compared with ANGPTL3
352 and APOC3 by cis-pQTL MR of the 694 FinnGen and UK Biobank endpoints using the *ANGPTL3*
353 c.*52_*60del and *APOC3* c.55+1G>A. Genetically lowered plasma ANGPTL3 levels were associated
354 with a reduced risk of being prescribed statin medication, two lipid-related diagnosis codes but not any
355 other patient-related outcome (**Supplemental Figure 4A**). *APOC3 c.55+1G>A* was associated with a
356 reduced risk of statin prescription but not any other endpoint (**Supplemental Figure 4B**).

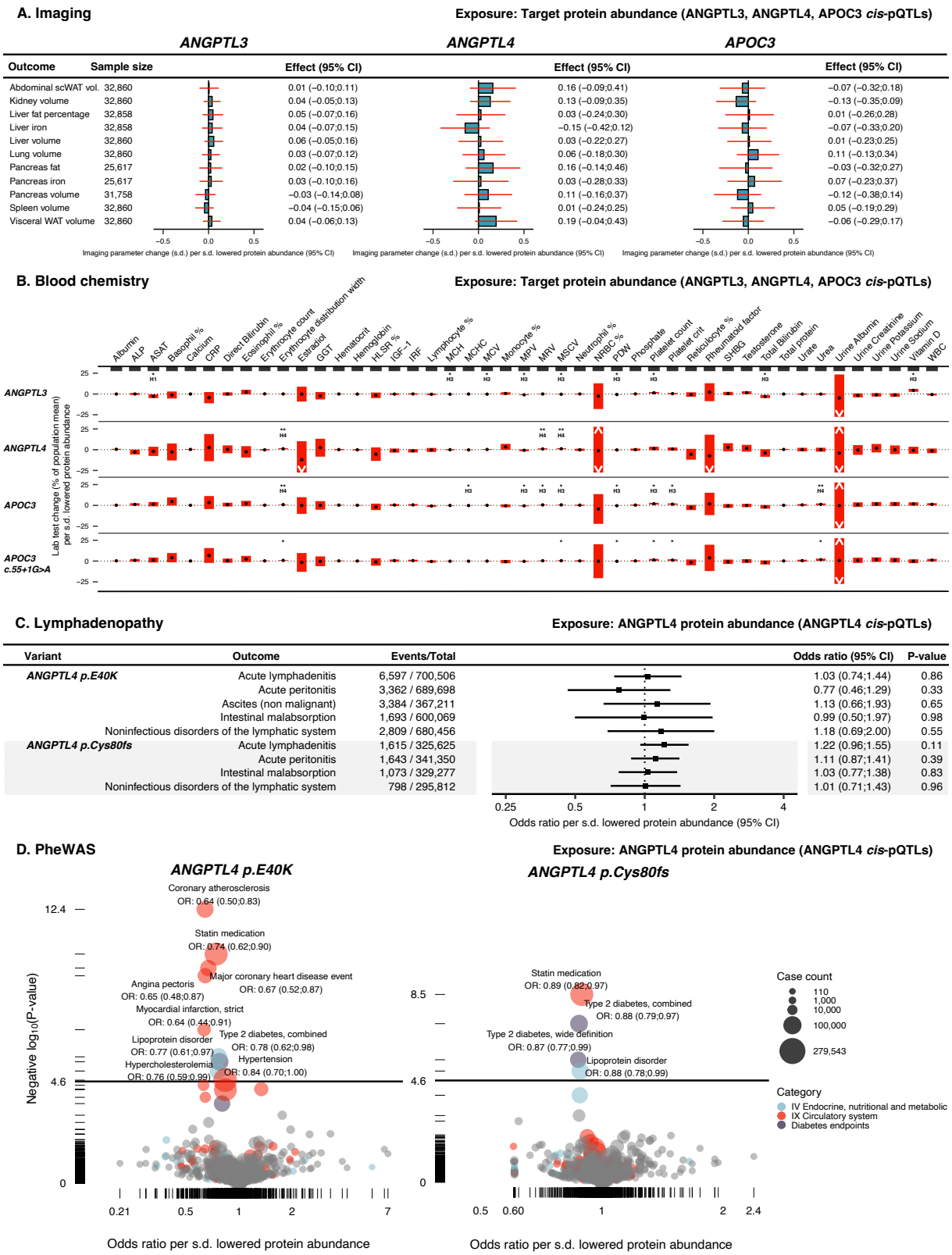

Figure 4. Results of MR analysis of potential adverse effects.
A: *Cis*-pQTL MR results on the imaging outcomes. Bar plots and red lines indicate the effect and 95% CI:s. 'scWAT' indicates subcutaneous white adipose tissue. 'vol.' indicates volume. **B:** *Cis*-pQTL MR of the clinical laboratory outcomes. The red bars indicate the 95 % CI. The black dots indicate the effect point estimate. * indicate $P < 0.05$. ** indicates $P < 0.05$ with a shared causal variant (H_4). A list explaining the abbreviations is provided in the supplemental material (**Table S1**). **Supplemental Figure 5** shows the results on a 1-s.d. scale. **C:** Results of ANGPTL4 *cis*-pQTL MR of mesenteric lymphadenopathy and malabsorption-related phenotypes. **D:** Volcano plot displaying the results of ANGPTL4 *cis*-pQTL phenome-wide MR scans on

694 outcomes in the FinnGen and UK Biobank meta-analysis (see **Table 2** and **Supplemental Table 1** for the reference and link to data, respectively). The *y*-axis solid straight lines indicate the phenome-wide significance threshold.

367 **Step 3**

368 **Common variants in *ANGPTL3*, *ANGPTL4*, and *APOC3* share their metabolic fingerprint with**
369 **deleterious variants**

370 In line with a previous investigation (45), we found no significant association between ANGPTL3
371 inactivation via common variants and CAD. Previously, however, evidence was presented that
372 deleterious variants in *ANGPTL3* are associated with a decreased risk of CAD (46, 47). As the common
373 variants adjacent to *ANGPTL3* only modestly impacted plasma lipids, it could be argued that they do
374 not accurately reflect the effects of more profound *ANGPTL3* inactivation. Therefore, we examined
375 whether common variants adjacent to *ANGPTL3*, *ANGPTL4*, and *APOC3* mimicked the effects (that is,
376 showed the same effect directionality) of deleterious variants.

377 All common variants adjacent to *ANGPTL3*, *ANGPTL4*, and *APOC3* were highly concordant with
378 deleterious variants within the same gene (**Figure 5A-C**). One hundred sixty-seven metabolite
379 associations near *ANGPTL3* showed a high concordance metric (R^2) of 84% between the common
380 variants and deleterious models. *ANGPTL4* common variants were also highly concordant with
381 *ANGPTL4* deleterious variants, having an R^2 of 86%. *APOC3* showed a concordance metric R^2 of 87%.
382 These results demonstrate that the common genetic variations adjacent to *ANGPTL3*, *ANGPTL4,* and
383 *APOC3* would be valid genetic instruments reflecting a modest "knock-down" of each respective gene.
384

385 **Comparative drug-target MR of LPL and endothelial lipase (EL) reveals that in order to achieve**
386 **CAD benefits, ANGPTL3 inhibition should primarily target LPL rather than EL**

387 ANGPTL3 targets both EL and LPL and may thus influence CAD via two independent pathways (48).
388 To compare the effects of these two target enzymes, we analyzed the effects of genetically instrumented
389 EL and LPL activity on CAD by performing functional-variant limited MR of the *LIPG* (encoding EL)
390 and *LPL* genes. We used the preferred enzyme substrate as the exposure, as EL prefers lipoprotein
391 phospholipids, whereas LPL primarily hydrolyzes lipoprotein TGs (49). We detected two functional
392 *LPL* variants and four functional *LIPG* variants with small to large effects on plasma TG/lipoprotein
393 phospholipids (range: 0.02 – 0.6 s.d. per allele).

394 MR analysis of *LPL* and *LIPG* found opposing significant associations with CAD for LPL (IVW meta-
395 analysis: OR: 0.74, $P=1\times10^{-4}$) and EL (IVW meta-analysis OR: 1.38, $P=5\times10^{-7}$) (**Figure 5D**). These
396 findings suggest that increased activity of LPL protects against the development of atherosclerosis,
397 whereas heightened activity of EL may contribute to the acceleration of atherosclerosis. The contrasting
398 impact of genetic EL and LPL activity on CAD risk suggests that for ANGPTL3 inactivation to lower
399 CAD risk, it may need to have a greater impact on LPL activity compared to EL activity.

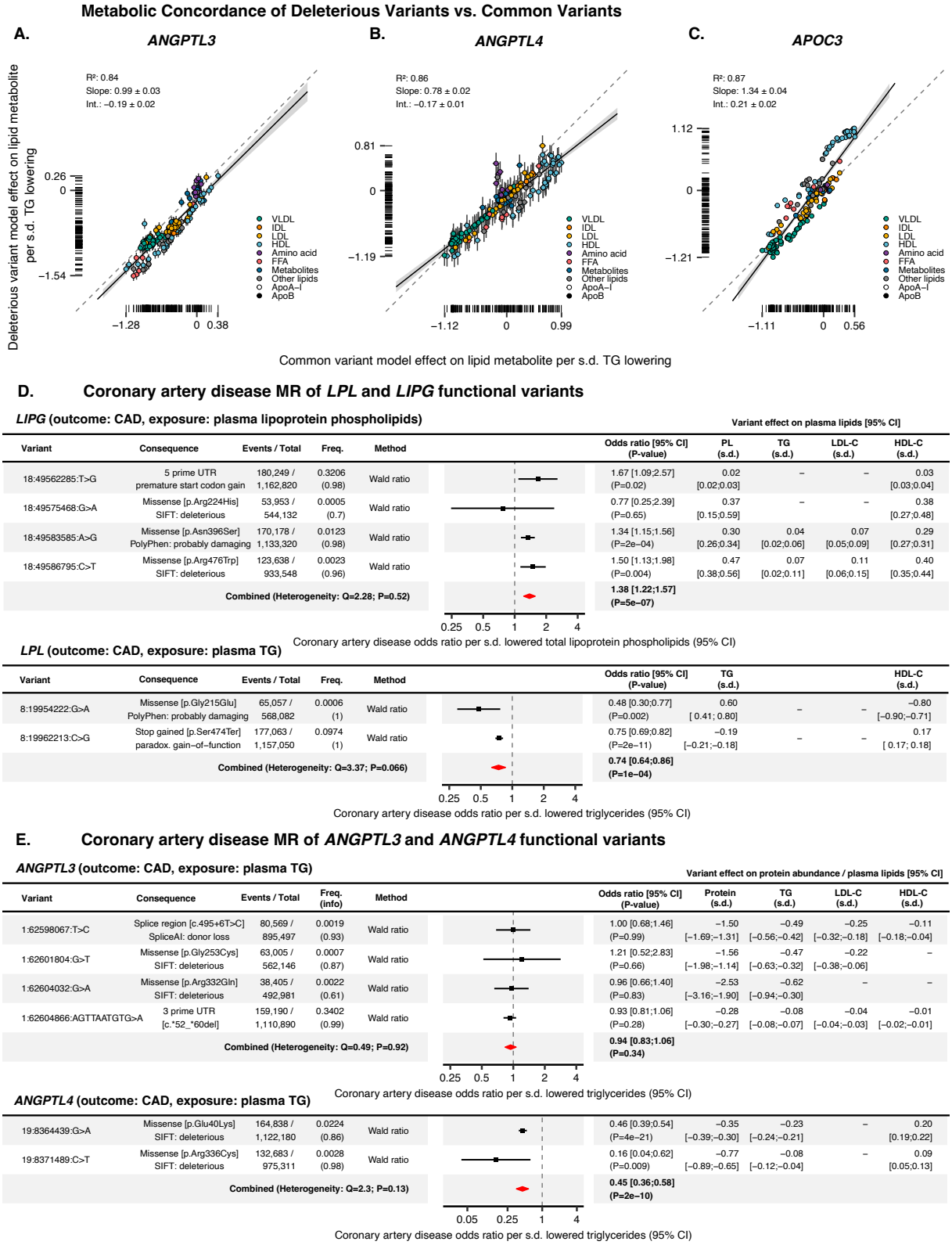

Figure 5. Results of validation analyses.
The concordance between the effect directionality of CVs and PTVs is displayed using scatter plots with a regression line. **A:** Comparison of the effect directionality between *ANGPTL3* CVs and PTVs. **B:** *ANGPTL4* CVs vs. PTVs. **C:** *APOC3* CVs vs. PTVs. 'R²' represents the coefficient of determination. 'Int.' indicates the regression line intercept. The color of the scattered dots indicates the lipid class of the NMR parameter. The collapsing model estimates were scaled by their 1-s.d. effect on plasma TGs to improve interpretability. **D:** Forest plots and tables showing the results of the CAD MR analysis focusing on functional variants in *LPL* and *LIPG*. Genetic association summary statistics of *LIPG* with the exposure were extracted from the UK biobank NMR study of 115,078 individuals retrieved from (36). *LPL* variant associations were retrieved from the same data set.

409 CAD data was from the Aragam et al. meta-analysis (30). **E:** Forest plots and tables showing the results of the CAD MR
410 analysis that limited the selection of genetic instruments to functional variants in *ANGPTL3* and *ANGPTL4*. "Freq." represents
411 the alternative allele frequency. "info" represents the imputation quality metric derived from the outcome GWAS. Variant effects
412 on plasma lipids were retrieved from (23). The *ANGPTL4* p.Glu40Lys (p.E40K) estimates differ slightly from *Figure 2* because a
413 slightly different estimator and UK Biobank subcohort were used to measure the association between the functional variants and
414 plasma TGs.

415 **Step 4**

416 **Deleterious variants in *ANGPTL3*, *ANGPTL4*, and *APOC3*, and the risk of CAD**

417 Two previous studies found that deleterious variants in *ANGPTL3* protected against CAD (3, 46). In an
418 effort to reproduce these findings, we performed a sensitivity MR analysis of CAD and limited the
419 selection of genetic instruments to functional variants. Functional annotations were detected for four
420 *ANGPTL3*, two *ANGPTL4*, and one *APOC3* variant. The detected *APOC3* variant was the *c.55+1G>A*
421 splice donor loss variant, which was already reported in **Figures 2-4**. The other variants associated with
422 lowered protein levels and triglycerides, with effect sizes ranging from profound to modest (protein
423 range: -2.53– -0.28; TG range -0.28– -0.62) (**Figure 5E**) (22). The variants were analyzed individually
424 and together using random-effects IVW meta-analysis. *Cis*-pQTL MR of the *ANGPTL3* variants
425 indicated that ANGPTL3 protein levels were not significantly associated with CAD, individually or
426 together (meta-analysis IVW OR per s.d. TG: 0.94, P=0.34) (**Figure 5E**). By contrast, reduced
427 *ANGPTL4* protein levels were associated with a decreased risk of CAD (meta-analysis IVW OR: 0.45
428 per s.d. TG, $P=2\times10^{-10}$) (**Figure 5E**).

429 Considering the beneficial effects of ANGPTL3, ANGPTL4, and APOC3 on plasma lipids, it was
430 expected that genetic inactivation of these proteins would confer protection against CAD. However, the
431 ANGPTL3 MR analyses focusing on common variants and MR of functional variants (identified
432 through DNA microarrays) did not support this hypothesis. Therefore, we pursued a meta-analysis of
433 DNA sequencing-based studies that studied the effect of *ANGPTL3*, *ANGPTL4*, and *APOC3* deleterious
434 variants on CAD. The rationale for excluding DNA microarray and exome bead chip-based studies was
435 the potential risk of introducing measurement error for rare variants (50, 51), leading to bias towards the
436 null hypothesis. DNA-sequencing-based substudies from previous papers (3, 46, 52, 53), were extracted
437 and analyzed together with genetic association analyses conducted in the UK Biobank. Loss-of-function
438 variant genetic association effect sizes typically range from -1 to -3 s.d. for their affected protein (22).
439 The carrier status of deleterious variants was associated with substantial decreases in protein levels for
440 both *ANGPTL3* (-1.29 s.d. protein, $P=9\times10^{-32}$) and *ANGPTL4* (-1.33 s.d. protein, $P=1.4\times10^{-43}$). APOC3
441 protein levels were not measured in the UK Biobank. However, *APOC3* deleterious variants were
442 associated with a significant reduction in TG (-0.68 mmol/L TG, $P=1\times10^{-82}$). .

443 The results of the meta-analysis are presented in **Figure 6**. The presence of *ANGPTL3* deleterious
444 variants was associated with reduced CAD risk (meta-analysis IVW OR: 0.41 per TG, $P=3\times10^{-5}$).
445 *ANGPTL4* deleterious variant carrier status, excluding p.E40K, was also associated with a reduced risk
446 of CAD (meta-analysis IVW OR: 0.32 per TG, P=0.016), as was *APOC3* deleterious variant carriers
447 status (meta-analysis IVW OR: 0.70 per TG, P=0.005). The key finding was the robust association of
448 *ANGPTL3* deleterious carrier status with a reduced risk of CAD. This association was not detected with
449 the other approaches and implies that ANGPTL3 lowering might offer atheroprotective benefits similar
450 to ANGPTL4 or APOC3 lowering.

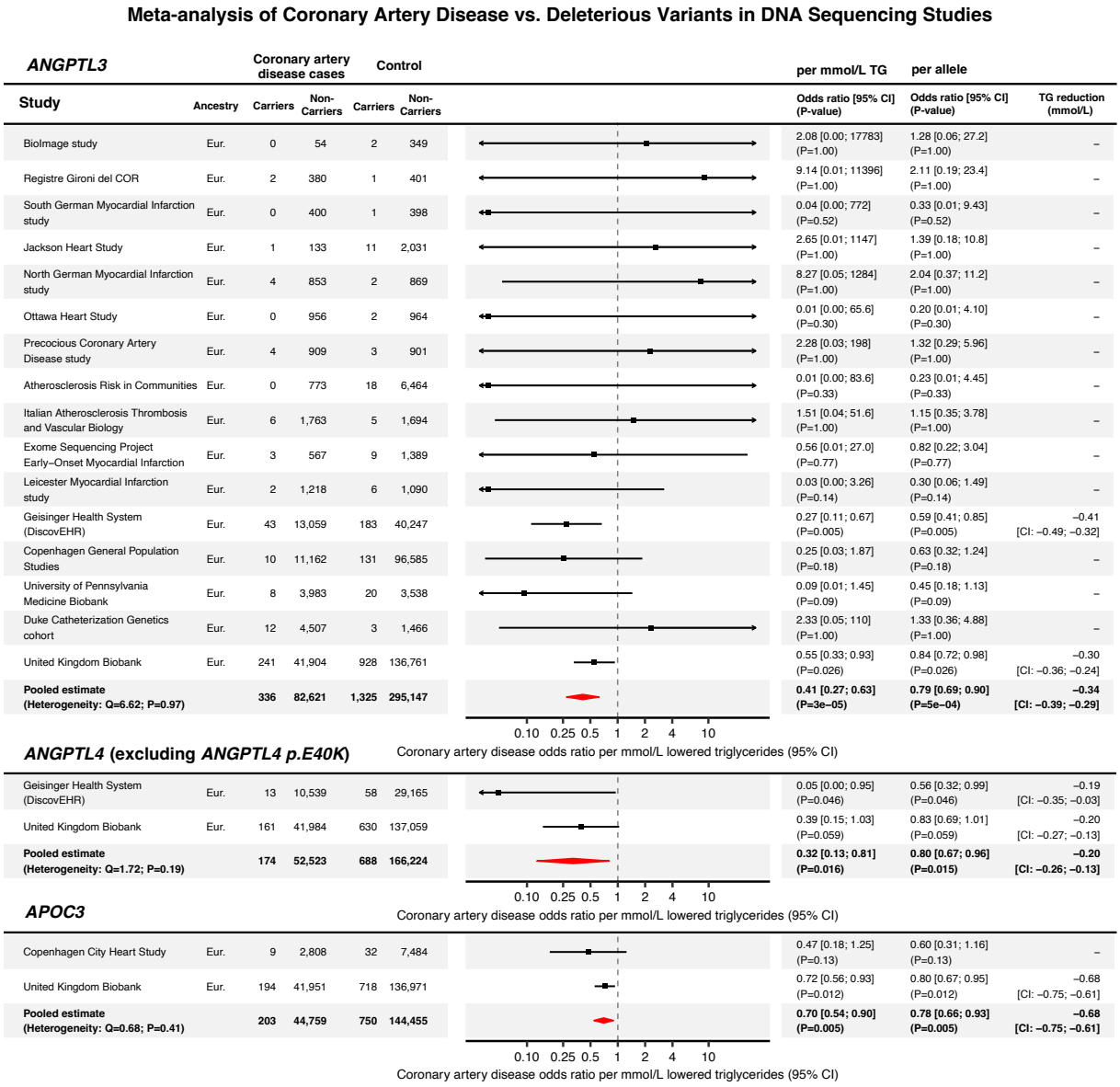

Figure 6. Meta-analysis of deleterious variants in ANGPTL3, ANGPTL4, and APOC3, and the risk of CAD. Forest plots and tables indicating the effect on CAD per mmol/L TG, and per allele. The deleterious variant effect estimates for each substudy were retrieved from (3, 23, 46, 52, 53). The case definition used in the Copenhagen City Heart Study was not exclusively restricted to CAD. 21% of the ischemic vascular disease cases were diagnosed with atherosclerotic cerebrovascular disease, rather than CAD (with CAD encompassing 79 % of the cases) (53). 'Eur.' denotes European ancestry.

457 **DISCUSSION**

458 We find that targeted inactivation and associated lowering of plasma APOC3 levels is predicted to
459 decrease plasma TG and LDL and raise HDL levels. Targeted lowering of plasma ANGPTL3 is expected
460 to reduce plasma TG, LDL, and HDL levels, while lowering of plasma ANGPTL4 is predicted to
461 decrease plasma TG and increase HDL levels. Based on these findings, it is expected that genetic
462 inactivation of APOC3, ANGPTL3, and ANGPTL4 levels is associated with protection against CAD.
463 Through MR and a meta-analysis of rare variant genetic association studies, we confirmed that targeted
464 inactivation and lowering of ANGPTL3, ANGPTL4, and APOC3 is associated with a lowered risk of
465 CAD. In addition, lifetime genetic lowering of ANGPTL4 was observed to reduce the risk of T2D,
466 indicating that ANGPTL4 inhibition might provide additional benefits to patients with T2D and
467 dyslipidemia.

468 The inactivation of ANGPTL4 in mice and monkeys was shown to lead to mesenteric lymphadenopathy
469 and other severe complications. Naturally, these observations raised serious concerns about the safety
470 of pharmacological targeting of ANGPTL4. Here, we did not find an association between genetic
471 ANGPTL4 inactivation and several disease codes related to lymphatic disorders. While these data do
472 not entirely exclude any harmful effects of ANGPTL4 inactivation, they do mitigate safety concerns
473 about the impact of whole-body inactivation of ANGPTL4 in humans. Recently, it was shown that
474 silencing of ANGPTL4 in the liver and adipose tissue using ASO markedly reduces plasma TG levels
475 in mice yet does not lead to mesenteric lymphadenopathy or other complications (16). These data
476 suggest that liver- and adipose tissue-specific inactivation of ANGPTL4 may confer similar
477 cardiovascular benefits as whole-body ANGPTL4 inactivation without any particular safety risks.

478 The association of ANGPTL4 with T2D was distinct from the other proteins that inhibit LPL. In
479 preclinical studies, mice overexpressing LPL in muscle were more insulin resistant, while mice lacking
480 LPL in muscle were more insulin sensitive. In contrast, mice overexpressing LPL in adipocytes were
481 more insulin sensitive (54, 55). The protective effect of enhanced LPL action in adipose tissue may be
482 related to increased lipid partitioning into the adipose tissue and reduced ectopic fat. While ANGPTL3,
483 ANGPTL4, and APOC3 all act through LPL, only ANGPTL4 acts exclusively via LPL, which may
484 explain why only genetic variation in ANGPTL4 is associated with T2D risk.

485 Previous studies reported conflicting findings regarding the association between ANGPTL3 and CAD.
486 Dewey et al. (3), and Stitziel et al. (46) found that rare deleterious *ANGPTL3* variants were associated
487 with decreased odds of ASCVD, whereas MR studies of common ANGPTL3-lowering variants reported
488 negative findings (45). By meta-analysis of deleterious variant genetic association studies, we found
489 clear, statistically robust evidence that lifetime genetic inactivation of ANGPTL3 confers protection
490 against CAD. These findings align with recent case reports indicating that ANGPTL3 lowering with
491 Evinacumab protects against atherosclerosis progression in HoFH patients (11, 12). A recent and similar
492 UK Biobank study examining the impact of protein-truncating *ANGPTL3* variants on CAD found no
493 association (56). Compared to their analysis, key differences were a broader case definition, a stricter

494 definition of controls, the inclusion of deleterious missense variants, and the meta-analysis, which
495 incorporated evidence from previous studies. These methodological differences strengthened statistical
496 power in our study, making a false negative finding less probable.
497 The discrepancy between the deleterious and common ANGPTL3 variants in terms of their association
498 with CAD could be due to a range of different factors. One possible explanation is the pleiotropic effects
499 of ANGPTL3. Besides inhibiting LPL, ANGPTL3 inhibits endothelial lipase (EL) (57). In a recent
500 paper, we showed that the LPL-independent effects of ANGPTL3 inactivation on plasma metabolic
501 parameters showed a striking inverse resemblance with EL inactivation, suggesting that ANGPTL3
502 modulates plasma lipid levels by inhibiting LPL and EL (41). Here, using MR, we compared the effects
503 of genetically instrumented EL and LPL activity on CAD. Whereas increased LPL activity reduced the
504 odds of CAD, increased EL activity increased the odds of CAD. The observed link between EL and
505 CAD is consistent with previous human genetic studies showing the possible harmful effects of a
506 genetically predicted increase in EL activity (58, 59). This suggests that ANGPTL3's interaction with
507 EL might counteract its cardiovascular benefits achieved through LPL inhibition under certain
508 physiological conditions. While our research demonstrated metabolic concordance between ANGPTL3
509 common variants and deleterious variants, it remains possible that more profound ANGPTL3
510 inactivation by deleterious variants could tip the balance in favor of LPL inhibition over EL. This shift
511 could potentially enhance the anti-atherosclerotic benefits of ANGPTL3 lowering.
512 Interestingly, the association of ANGPTL3 inactivation with CAD was only present for rare deleterious
513 variants when the carrier status was determined by DNA sequencing. This exposes the limitations of
514 drug-target MR studies using DNA micro-array-based GWAS. When rare variants are incorrectly
515 imputed, this typically introduces a one-sided loss of information that biases toward the null hypothesis,
516 leading to falsely negative findings (51). Even though the imputation quality score (e.g., 'INFO') reports
517 an imputation quality metric, this metric does not really measure the true imputation accuracy (60). The
518 imputation accuracy can only truly be determined if variant carrier status is called by genotyping (e.g.,
519 via DNA sequencing). However, studying rare variants in genetic association studies is not without
520 drawbacks. An important limitation of rare variants is statistical imprecision simply due to their rarity
521 (61). Rare variants also often emerged relatively recently and consequently are more susceptible to
522 confounding by enrichment in specific geographical regions, families, or socioeconomic strata (62).
523 Even if appropriate model adjustments are applied, subtle differences in population structure could cause
524 a small number of extra alleles to be present in the control (or case) group. This can lead to biased
525 estimates when the rare alternative allele is present in ten, or hundred individuals in total, which is often
526 the case for rare variant studies even when the total sample size is above hundreds of thousands. Overall,
527 our findings underscore the importance of combining evidence from rare deleterious and benign
528 common variants in genetic association studies of complex disease phenotypes.
529 The complexity of the *APOA1-APOA5-APOC3* locus and the potential confounding due to LD poses
530 significant challenges in separating the genetic association signals. The use of *APOC3* c.55+1G>A as a

531 genetic instrument was justified because of its independence from common variants within this region,
532 making it ideal for studying APOC3 inactivation specifically. On the other hand, the analyses of APOC3
533 inactivation that did not include the c.55+1G>A variant should be interpreted with caution. Compared
534 to clinical trials, MR analysis can exaggerate the magnitude of the effect of inactivating a gene/protein
535 (63). Cis-pQTL MR utilizing protein-coding variants warrants extra carefulness due to the possibility of
536 epitope-binding artifacts, which may complicate the precise interpretation of effect sizes. The p.E40K
537 coding variant was the only variant qualifying as a *cis*-pQTL in the *ANGPTL4* region in the Step 1-2
538 analyses. While our validation analyses suggested this specific association was not attributable to
539 epitope-binding artifacts, we still advise caution when extrapolating effect sizes from the analyses.
540 Additionally, MR and other genetic association studies estimate lifelong exposure to changed gene
541 function, while drug trials typically last 2–5 years in late adulthood. If the treatment effect
542 multiplicatively interacts with time, MR may exaggerate it. This constraint should be considered when
543 translating MR findings to predict the results of clinical trials. For ANGPTL4, Dewey et al. (52), found
544 that the TG levels of p.E40K homozygotes were reduced by 0.58 mmol/L (0.92 mmol/L for p.E40K
545 homozygotes vs. 1.49 mmol/L in non-carriers; relative change -39%) in a normotriglyceridemic
546 population. When translating these findings (TG reduction of 0.58 mmol/L) onto the effect size on CAD
547 found in this study, one would expect that lifetime *ANGPTL4* inactivation—in a population of
548 normotriglyceridemic individuals—results in a risk reduction corresponding to a CAD odds ratio of 0.61
549 (95% CI: 0.52–0.72).
550 In conclusion, our genetic analysis predicts that in a broader dyslipidemic patient population, therapies
551 aimed at decreasing plasma ANGPTL3, ANGPTL4, or APOC3 levels will be effective in preventing
552 CAD without raising specific safety concerns. In addition, therapies aimed at reducing plasma levels of
553 ANGPTL4 may provide additional benefits to patients with dyslipidemia and T2D.

ETHICAL REVIEW

This study analyzed scientific data that is available to the public, as detailed in **Table 1** and **Supplemental Table 1**, where references to the specific datasets can be found. Analyses using individual-level access to the UK Biobank Resource were conducted under Application Number #148828. The Erasmus Rucphen Family study was approved by the medical ethics board of the Erasmus MC Rotterdam, the Netherlands (64). All studies complied with the ethical standards outlined in the Helsinki Declaration.

ACKNOWLEDGEMENTS

We would like to thank Prof. Cornelia van Duijn and Prof. Ko Willems van Dijk for providing access to samples from the Erasmus Rucphen Family study. We would like to thank the participants and researchers of the CARDIoGRAMplusC4D, CKDGen, deCODE, DIAGRAM, EPIC-CVD, FinnGen, GIGASTROKE, GLGC, and UK biobank studies, as well as the other non-consortium studies.

FUNDING

This research received no specific grants from public or non-profit funding agencies.

CONFLICT OF INTEREST

F.L. is a part-time employee of Lipigon Pharmaceuticals AB. S.K.N. is the chief executive officer of Lipigon. S.K. is a paid consultant for Lipigon.

DATA AVAILABILITY STATEMENT

Database identifiers and links to the public data sets are provided in **Supplemental Table 1**. Access to UK Biobank data is limited to authorized researchers who comply with data use policies to safeguard participant confidentiality. Interested researchers must apply to UK Biobank, adhering to an application process that ensures ethical and legal compliance in data handling. UK Biobank data set identifiers used for the analyses under Application Number #148828 are provided in the **Supplemental Methods**. The data from the Erasmus Rucphen Family study (ERF) cannot be shared publicly due to data protection laws. Access to this data is restricted to ensure participant confidentiality, aligning with legal and ethical obligations. Any request for access to the data for legitimate scientific purposes can be directed to the principal investigators of the ERF study, subject to a rigorous review process ensuring that all legal and ethical standards are met. The analyses in this manuscript were performed using the R programming language (v.4.2.1) with the packages coloc, cowplot, data.table, ggplot2, ggthemes, mungegwas, phewas, twosamplemr, wesanderson, writexl, and the Python programming language (v.3.8.16) using the packages numpy, pandas, and scipy. The LD matrix estimates were calculated using PLINK (v1.90b6.24).

REFERENCES

1. Tardif JC, Karwatowska-Prokopczuk E, Amour ES, Ballantyne CM, Shapiro MD, Moriarty PM, et al. Apolipoprotein C-III reduction in subjects with moderate hypertriglyceridaemia and at high cardiovascular risk. Eur Heart J. 2022;43(14):1401-12.
2. Ahmad Z, Banerjee P, Hamon S, Chan KC, Bouzelmat A, Sasiela WJ, et al. Inhibition of Angiopoietin-Like Protein 3 With a Monoclonal Antibody Reduces Triglycerides in Hypertriglyceridemia. Circulation. 2019;140(6):470-86.
3. Dewey FE, Gusarova V, Dunbar RL, O'Dushlaine C, Schurmann C, Gottesman O, et al. Genetic and Pharmacologic Inactivation of ANGPTL3 and Cardiovascular Disease. N Engl J Med. 2017;377(3):211-21.
4. Gaudet D, Gipe DA, Pordy R, Ahmad Z, Cuchel M, Shah PK, et al. ANGPTL3 Inhibition in Homozygous Familial Hypercholesterolemia. N Engl J Med. 2017;377(3):296-7.
5. Raal FJ, Rosenson RS, Reeskamp LF, Hovingh GK, Kastelein JJP, Rubba P, et al. Evinacumab for Homozygous Familial Hypercholesterolemia. N Engl J Med. 2020;383(8):711-20.
6. Rosenson RS, Burgess LJ, Ebenbichler CF, Baum SJ, Stroes ESG, Ali S, et al. Evinacumab in Patients with Refractory Hypercholesterolemia. N Engl J Med. 2020;383(24):2307-19.
7. Gaudet D, Karwatowska-Prokopczuk E, Baum SJ, Hurh E, Kingsbury J, Bartlett VJ, et al. Vupanorsen, an N-acetyl galactosamine-conjugated antisense drug to ANGPTL3 mRNA, lowers triglycerides and atherogenic lipoproteins in patients with diabetes, hepatic steatosis, and hypertriglyceridaemia. Eur Heart J. 2020;41(40):3936-45.
8. Graham MJ, Lee RG, Brandt TA, Tai LJ, Fu W, Peralta R, et al. Cardiovascular and Metabolic Effects of ANGPTL3 Antisense Oligonucleotides. N Engl J Med. 2017;377(3):222-32.
9. Watts GF, Schwabe C, Scott R, Gladding P, Sullivan D, Baker J, et al. Abstract 15751: Pharmacodynamic Effect of ARO-ANG3, an Investigational RNA Interference Targeting Hepatic Angiopoietin-like Protein 3, in Patients With Hypercholesterolemia. Circulation. 2020;142(Suppl_3):A15751-A.
10. Bergmark BA, Marston NA, Bramson CR, Curto M, Ramos V, Jevne A, et al. Effect of Vupanorsen on Non-High-Density Lipoprotein Cholesterol Levels in Statin-Treated Patients With Elevated Cholesterol: TRANSLATE-TIMI 70. Circulation. 2022;145(18):1377-86.
11. Reeskamp LF, Nurmohamed NS, Bom MJ, Planken RN, Driessen RS, van Diemen PA, et al. Marked plaque regression in homozygous familial hypercholesterolemia. Atherosclerosis. 2021;327:13-7.
12. Khoury E, Lauzière A, Raal FJ, Mancini J, Gaudet D. Atherosclerotic plaque regression in homozygous familial hypercholesterolaemia: a case report of a long-term lipid-lowering therapy involving LDL-receptor-independent mechanisms. Eur Heart J Case Rep. 2023;7(1):ytad029.
13. Desai U, Lee EC, Chung K, Gao C, Gay J, Key B, et al. Lipid-lowering effects of anti-angiopoietin-like 4 antibody recapitulate the lipid phenotype found in angiopoietin-like 4 knockout mice. Proc Natl Acad Sci U S A. 2007;104(28):11766-71.
14. Lichtenstein L, Mattijssen F, de Wit NJ, Georgiadi A, Hooiveld GJ, van der Meer R, et al. Angptl4 protects against severe proinflammatory effects of saturated fat by inhibiting fatty acid uptake into mesenteric lymph node macrophages. Cell Metab. 2010;12(6):580-92.
15. Oteng AB, Bhattacharya A, Brodesser S, Qi L, Tan NS, Kersten S. Feeding Angptl4-/- mice trans fat promotes foam cell formation in mesenteric lymph nodes without leading to ascites. J Lipid Res. 2017;58(6):1100-13.
16. Deng M, Kutrolli E, Sadewasser A, Michel S, Joibari MM, Jaschinski F, et al. ANGPTL4 silencing via antisense oligonucleotides reduces plasma triglycerides and glucose in mice without causing lymphadenopathy. J Lipid Res. 2022;63(7):100237.
17. Davies BSJ. Can targeting ANGPTL proteins improve glucose tolerance? Diabetologia. 2018;61(6):1277-81.
18. Burgess S, Dudbridge F, Thompson SG. Combining information on multiple instrumental variables in Mendelian randomization: comparison of allele score and summarized data methods. Stat Med. 2016;35(11):1880-906.
19. Schmidt AF, Finan C, Gordillo-Marañón M, Asselbergs FW, Freitag DF, Patel RS, et al. Genetic drug target validation using Mendelian randomisation. Nat Commun. 2020;11(1):3255.
20. Timpson NJ, Walter K, Min JL, Tachmazidou I, Malerba G, Shin SY, et al. A rare variant in APOC3 is associated with plasma triglyceride and VLDL levels in Europeans. Nat Commun. 2014;5:4871.
21. Ferkingstad E, Sulem P, Atlason BA, Sveinbjornsson G, Magnusson MI, Styrmisdottir EL, et al. Large-scale integration of the plasma proteome with genetics and disease. Nat Genet. 2021;53(12):1712-21.
22. Dhindsa RS, Burren OS, Sun BB, Prins BP, Matelska D, Wheeler E, et al. Rare variant associations with plasma protein levels in the UK Biobank. Nature. 2023;622(7982):339-47.
23. Wang Q, Dhindsa RS, Carss K, Harper AR, Nag A, Tachmazidou I, et al. Rare variant contribution to human disease in 281,104 UK Biobank exomes. Nature. 2021;597(7877):527-32.
24. Kurki MI, Karjalainen J, Palta P, Sipilä TP, Kristiansson K, Donner KM, et al. FinnGen provides genetic insights from a well-phenotyped isolated population. Nature. 2023;613(7944):508-18.
25. Sudlow C, Gallacher J, Allen N, Beral V, Burton P, Danesh J, et al. UK biobank: an open access resource for identifying the causes of a wide range of complex diseases of middle and old age. PLoS Med. 2015;12(3):e1001779.
26. Slatkin M. Linkage disequilibrium--understanding the evolutionary past and mapping the medical future. Nat Rev Genet. 2008;9(6):477-85.
27. Zuber V, Grinberg NF, Gill D, Manipur I, Slob EAW, Patel A, et al. Combining evidence from Mendelian randomization and colocalization: Review and comparison of approaches. Am J Hum Genet. 2022;109(5):767-82.

28. Giambartolomei C, Vukcevic D, Schadt EE, Franke L, Hingorani AD, Wallace C, et al. Bayesian test for colocalisation between pairs of genetic association studies using summary statistics. PLoS Genet. 2014;10(5):e1004383.
29. Abraham W. The Fitting of Straight Lines if Both Variables are Subject to Error. The Annals of Mathematical Statistics. 1940;11(3):284-300.
30. Aragam KG, Jiang T, Goel A, Kanoni S, Wolford BN, Atri DS, et al. Discovery and systematic characterization of risk variants and genes for coronary artery disease in over a million participants. Nat Genet. 2022;54(12):1803-15.
31. Wuttke M, Li Y, Li M, Sieber KB, Feitosa MF, Gorski M, et al. A catalog of genetic loci associated with kidney function from analyses of a million individuals. Nat Genet. 2019;51(6):957-72.
32. Mishra A, Malik R, Hachiya T, Jürgenson T, Namba S, Posner DC, et al. Stroke genetics informs drug discovery and risk prediction across ancestries. Nature. 2022;611(7934):115-23.
33. Ghodsian N, Abner E, Emdin CA, Gobeil É, Taba N, Haas ME, et al. Electronic health record-based genome-wide meta-analysis provides insights on the genetic architecture of non-alcoholic fatty liver disease. Cell Rep Med. 2021;2(11):100437.
34. Mahajan A, Taliun D, Thurner M, Robertson NR, Torres JM, Rayner NW, et al. Fine-mapping type 2 diabetes loci to single-variant resolution using high-density imputation and islet-specific epigenome maps. Nat Genet. 2018;50(11):1505-13.
35. Nag A, Dhindsa RS, Middleton L, Jiang X, Vitsios D, Wigmore E, et al. Effects of protein-coding variants on blood metabolite measurements and clinical biomarkers in the UK Biobank. Am J Hum Genet. 2023;110(3):487-98.
36. Elsworth B, Lyon M, Alexander T, Liu Y, Matthews P, Hallett J, et al. The MRC IEU OpenGWAS data infrastructure. bioRxiv. 2020:2020.08.10.244293.
37. Evangelou E, Warren HR, Mosen-Ansorena D, Mifsud B, Pazoki R, Gao H, et al. Genetic analysis of over 1 million people identifies 535 new loci associated with blood pressure traits. Nat Genet. 2018;50(10):1412-25.
38. Pulit SL, Stoneman C, Morris AP, Wood AR, Glastonbury CA, Tyrrell J, et al. Meta-analysis of genome-wide association studies for body fat distribution in 694 649 individuals of European ancestry. Hum Mol Genet. 2019;28(1):166-74.
39. Stanzick KJ, Li Y, Schlosser P, Gorski M, Wuttke M, Thomas LF, et al. Discovery and prioritization of variants and genes for kidney function in >1.2 million individuals. Nat Commun. 2021;12(1):4350.
40. Liu Y, Basty N, Whitcher B, Bell JD, Sorokin EP, van Bruggen N, et al. Genetic architecture of 11 organ traits derived from abdominal MRI using deep learning. Elife. 2021;10.
41. Landfors F, Chorell E, Kersten S. Genetic Mimicry Analysis Reveals the Specific Lipases Targeted by the ANGPTL3-ANGPTL8 Complex and ANGPTL4. J Lipid Res. 2023;64(1):100313.
42. Wang Q, Oliver-Williams C, Raitakari OT, Viikari J, Lehtimaki T, Kahonen M, et al. Metabolic profiling of angiopoietin-like protein 3 and 4 inhibition: a drug-target Mendelian randomization analysis. Eur Heart J. 2021;42(12):1160-9.
43. McLaren W, Gil L, Hunt SE, Riat HS, Ritchie GR, Thormann A, et al. The Ensembl Variant Effect Predictor. Genome Biol. 2016;17(1):122.
44. Yin W, Romeo S, Chang S, Grishin NV, Hobbs HH, Cohen JC. Genetic variation in ANGPTL4 provides insights into protein processing and function. J Biol Chem. 2009;284(19):13213-22.
45. Richardson TG, Leyden GM, Wang Q, Bell JA, Elsworth B, Davey Smith G, et al. Characterising metabolomic signatures of lipid-modifying therapies through drug target mendelian randomisation. PLoS Biol. 2022;20(2):e3001547.
46. Stitziel NO, Khera AV, Wang X, Bierhals AJ, Vourakis AC, Sperry AE, et al. ANGPTL3 Deficiency and Protection Against Coronary Artery Disease. J Am Coll Cardiol. 2017;69(16):2054-63.
47. Musunuru K, Pirruccello JP, Do R, Peloso GM, Guiducci C, Sougnez C, et al. Exome sequencing, ANGPTL3 mutations, and familial combined hypolipidemia. N Engl J Med. 2010;363(23):2220-7.
48. Kovrov O, Kristensen KK, Larsson E, Ploug M, Olivecrona G. On the mechanism of angiopoietin-like protein 8 for control of lipoprotein lipase activity. J Lipid Res. 2019;60(4):783-93.
49. Jaye M, Lynch KJ, Krawiec J, Marchadier D, Maugeais C, Doan K, et al. A novel endothelial-derived lipase that modulates HDL metabolism. Nat Genet. 1999;21(4):424-8.
50. Cherukuri PF, Soe MM, Condon DE, Bartaria S, Meis K, Gu S, et al. Establishing analytical validity of BeadChip array genotype data by comparison to whole-genome sequence and standard benchmark datasets. BMC Med Genomics. 2022;15(1):56.
51. Stahl K, Gola D, König IR. Assessment of Imputation Quality: Comparison of Phasing and Imputation Algorithms in Real Data. Front Genet. 2021;12:724037.
52. Dewey FE, Gusarova V, O'Dushlaine C, Gottesman O, Trejos J, Hunt C, et al. Inactivating Variants in ANGPTL4 and Risk of Coronary Artery Disease. N Engl J Med. 2016;374(12):1123-33.
53. Jorgensen AB, Frikke-Schmidt R, Nordestgaard BG, Tybjaerg-Hansen A. Loss-of-function mutations in APOC3 and risk of ischemic vascular disease. N Engl J Med. 2014;371(1):32-41.
54. Kim JK, Fillmore JJ, Chen Y, Yu C, Moore IK, Pypaert M, et al. Tissue-specific overexpression of lipoprotein lipase causes tissue-specific insulin resistance. Proc Natl Acad Sci U S A. 2001;98(13):7522-7.
55. Walton RG, Zhu B, Unal R, Spencer M, Sunkara M, Morris AJ, et al. Increasing adipocyte lipoprotein lipase improves glucose metabolism in high fat diet-induced obesity. J Biol Chem. 2015;290(18):11547-56.
56. Gobeil É, Bourgault J, Mitchell PL, Houessou U, Gagnon E, Girard A, et al. Genetic inhibition of angiopoietin-like protein-3, lipids, and cardiometabolic risk. Eur Heart J. 2024;45(9):707-21.
57. Gusarova V, Alexa CA, Wang Y, Rafique A, Kim JH, Buckler D, et al. ANGPTL3 blockade with a human monoclonal antibody reduces plasma lipids in dyslipidemic mice and monkeys. J Lipid Res. 2015;56(7):1308-17.
58. Thomas DG, Wei Y, Tall AR. Lipid and metabolic syndrome traits in coronary artery disease: a Mendelian randomization study. J Lipid Res. 2021;62:100044.

59. Singaraja RR, Sivapalaratnam S, Hovingh K, Dubé MP, Castro-Perez J, Collins HL, et al. The impact of partial and complete loss-of-function mutations in endothelial lipase on high-density lipoprotein levels and functionality in humans. Circ Cardiovasc Genet. 2013;6(1):54-62.
60. Zheng HF, Rong JJ, Liu M, Han F, Zhang XW, Richards JB, et al. Performance of genotype imputation for low frequency and rare variants from the 1000 genomes. PLoS One. 2015;10(1):e0116487.
61. Zuk O, Schaffner SF, Samocha K, Do R, Hechter E, Kathiresan S, et al. Searching for missing heritability: designing rare variant association studies. Proc Natl Acad Sci U S A. 2014;111(4):E455-64.
62. Locke AE, Steinberg KM, Chiang CWK, Service SK, Havulinna AS, Stell L, et al. Exome sequencing of Finnish isolates enhances rare-variant association power. Nature. 2019;572(7769):323-8.
63. Burgess S, Butterworth A, Malarstig A, Thompson SG. Use of Mendelian randomisation to assess potential benefit of clinical intervention. BMJ. 2012;345:e7325.
64. Henneman P, Aulchenko YS, Frants RR, van Dijk KW, Oostra BA, van Duijn CM. Prevalence and heritability of the metabolic syndrome and its individual components in a Dutch isolate: the Erasmus Rucphen Family study. J Med Genet. 2008;45(9):572-7.
65. Jonker JT, Smit JW, Hammer S, Snel M, van der Meer RW, Lamb HJ, et al. Dietary modulation of plasma angiopoietin-like protein 4 concentrations in healthy volunteers and in patients with type 2 diabetes. Am J Clin Nutr. 2013;97(2):255-60.

745 **APPENDICES**

746

747 **Supplemental Note**

748 This document contains the **Supplemental Methods**. The supplemental note *.pdf* also contains
749 **Supplemental Figures *1–6***.

750

751 **Supplemental Figures**

752 *The Supplemental Figures 1–6 are contained within the supplemental note .pdf file.*

753 **Supplemental Figure 1. Scatter plots showing the results of the drug-target MR analyses.** Each
754 subplot represents the results of the analyses displayed in **Figures 2-4** of the main manuscript that
755 used more than one genetic instrument.

756 **Supplemental Figure 2. Regional genetic association plots showing the results of the**
757 **colocalization analyses.** Each subplot represents the results of the analyses displayed in **Figure 2-4** of
758 the main manuscript.

759 **Supplemental Figure 3. Results of cis-pQTL MR analyses of the estimated glomerular filtration**
760 **rate by (eGFR) by Cystatin C and plasma Creatinine.** The findings are displayed in bar graphs,
761 illustrating the level of the effect per s.d. decrease in protein abundance. The red lines represent the 95%
762 CI.

763 **Supplemental Figure 4. Results of phenome-wide MR analysis on FinnGen outcomes using**
764 ***ANGPTL3 rs34483103-1:62604866:AGTTAATGTG>A* [3 prime UTR, c.*52_*60del] and *APOC3***
765 ***rs138326449-11:116830638:G>A* [donor loss, c.55+1G>A] variants. A**: Volcano plot displaying the
766 results of ANGPTL3 cis-pQTL phenome-wide MR. **B**: APOC3 cis-pQTL phenome-wide MR volcano
767 plot. The y-axis solid straight lines indicate the phenome-wide significance threshold. 'OR' indicates
768 the odds ratio with 95% confidence intervals with Bonferroni correction for the 694 FinnGen
769 outcomes.

770 **Supplemental Figure 5. Cis-pQTL MR of the clinical laboratory outcomes, showing the results on**
771 **a 1-s.d. scale.** The red bars indicate the 95 % CI. The black dots indicate the effect point estimate. '*'
772 indicate $P < 0.05$. '**' indicates $P < 0.05$ with a shared causal variant (H_4). A list explaining the
773 abbreviations is provided in the supplemental material (**Supplemental Table 1**).

774 **Supplemental Figure 6. Wildtype human ANGPTL4 protein and the ANGPTL4 E40K variant**
775 **protein are detected to a similar extent by the antibody used in the human ANGPTL4 ELISA.**
776 Western blot of the precipitated medium of HEK293 cells transfected with expression vectors for
777 different mutant forms of human ANGPTL4 fused to a V5-tag (65). CC/AA is an oligomerization
778 defective ANGPTL4 variant. SDS-PAGE was performed using a loading buffer without DTT or other
779 disulfide-reducing agent. Equal amounts of medium were loaded. Membranes were blotted with an

antibody from R&D Systems that is used for the human ANGPTL4 Elisa (AF3485, 1:2500). Secondary antibody was goat anti-rabbit IgG conjugated to HRP (1:5000).

Supplemental Tables

The Supplemental Tables 1-10 are located within the supplemental_tables_1_10.xlsx file. The .xlsx file is available via a public repository and can be accessed via the following link: https://doi.org/10.5281/zenodo.10880711

Supplemental Table 1. Description of GWAS data sets

List of the GWAS data sets used. 'database.ID' denotes the EBI GWAS catalog identifiers if starting by "GCST", or the UK biobank showcase identifier if starting by a number.

Supplemental Table 2. MR results with 1000Genomes LD matrix

Results of the MR analyses that are presented in the paper. 'rsids.dbsnp.ver144' denote the rsids that were used in each MR model.

Supplemental Table 3. MR sensitivity analysis w. UKB 337K LD matrix vs. 1000Genomes.

LD matrix sensitivity analysis using the 1000Genomes and UKB 337K LD matrices.'heterogeneity.statistic' indicates the heterogeneity P-value, which is described in detail in the supplemental note.

Supplemental Table 4. MR sample overlap risk of bias analysis

Result of the risk of bias from sample overlap analysis reporting the F-statistics, bias ('Beta.bias.low.scenario', ' Beta.bias.medium.scenario', and ' Beta.bias.high.scenario') and type 1 error inflation (Type1error.lowbias.scenario, Type1error.mediumbias.scenario, Type1error.highbias.scenario) for each scenario and model.

Supplemental Table 5. ICD codes used for UKB lymphadenopathy-related phecodes

Phecode and ICD-codes as described in the Methods section.

Supplemental Table 6. ANGPTL4 p.40K pQTL MR PheWAS results

Detailed results of the MR analyses presented in **Figure 4D**.

Supplemental Table 7. ANGPTL4 p.Cys80fs pQTL MR PheWAS results

Detailed results of the MR analyses presented in **Figure 4D**.

Supplemental Table 8. *ANGPTL3 rs34483103-1:62604866:AGTTAATGTG>A* [3 prime UTR, c.*52_*60del] pQTL MR PheWAS results

Detailed results of the MR analyses presented in **Supplemental Figure 4A**.

Supplemental Table 9. *APOC3 rs138326449-11:116830638:G>A* [donor loss, c.55+1G>A] pQTL MR PheWAS results

Detailed results of the MR analyses presented in **Supplemental Figure 4B**.

Supplemental Table 10. List of variants used in the UK Biobank genetic association analyses

'rsID' indicates the NCBI Reference SNP cluster ID. 'REVEL' denotes the Rare Exome Variant Ensemble Learner pathogenicity prediction score for missense variants.